176
5/20/81

ornl

OAK
RIDGE
NATIONAL
LABORATORY

UNION CARBIDE

R4487

MASTER

ORNL/TM-7715

GCFR Plenum Shield Design—Exit Shield Experiment

F. J. Muckenthaler
J. L. Hull
J. J. Manning

OPERATED BY
UNION CARBIDE CORPORATION
FOR THE UNITED STATES
DEPARTMENT OF ENERGY

Printed in the United States of America. Available from
National Technical Information Service
U.S. Department of Commerce
5285 Port Royal Road, Springfield, Virginia 22161
NTIS price codes—Printed Copy: A05 Microfiche A01

ORNL/TM-7715
Distribution Category
UC-77

Contract No. W-7405-eng-26

ENGINEERING PHYSICS DIVISION

Gas-Cooled Reactor Programs
FTP/A 01351

Date Published: May 1981

GCFR PLENUM SHIELD DESIGN — EXIT SHIELD EXPERIMENT

F. J. Muckenthaler
J. L. Hull*
J. J. Manning

This Work Sponsored by
U. S. Department of Energy
Office of Advanced Nuclear Systems
and Projects

*Operations Division

OAK RIDGE NATIONAL LABORATORY
Oak Ridge, Tennessee 37830
operated by
UNION CARBIDE CORPORATION
for the
DEPARTMENT OF ENERGY

Report Written By:

F. J. Muckenthaler

Work Done By:

L. B. Holland*

J. L. Hull*

D. T. Ingersoll

J. O. Johnson†

J. J. Manning

F. J. Muckenthaler

J. W. Paul‡

Manuscript Prepared By:

E. S. Howe

M. H. Schulte

*Operations Division

‡Plant and Equipment Division

†Guest Student Assignee from the University of Tennessee, Knoxville

CONTENTS

LIST OF TABLES

LIST OF FIGURES

GCFR PLENUM SHIELD DESIGN — EXIT SHIELD EXPERIMENT*

F. J. Muckenthaler, J. L. Hull, and J. J. Manning

ABSTRACT

This report describes the integral flux, energy spectra, and dose rate measurements made for the Exit Shield Experiment at the Oak Ridge National Laboratory Tower Shielding Facility as part of the Gas Cooled Fast Breeder Reactor program. The source was the same mockup of fuel pins used in the previous Grid Plate Shield Experiment. Two mockups of the upper axial shield were studied: one with seven subassemblies prototypic of that portion of the Exit Shield without a control rod, and another that was representative of the shield region with a control rod.

The experiment was performed to provide verification of: the shield design methods, the shield effectiveness of a prototypic mockup, the analytical ability to calculate streaming effects in the presence of a control rod, and the source term bias factors for the upper plenum. A series of measurements were made behind each configuration; for those configurations containing the control rod, measurements were made as a function of control rod position with and without B_4C in the control rod's subassembly.

INTRODUCTION

An experiment was performed at the Tower Shielding Facility (TSF) to provide data against which the validity of the calculational methods used in the design of the exit shield for the proposed Gas Cooled Fast Breeder Reactor (GCFR)[1] could be tested. The exit shield, located directly above the axial blanket, was designed to minimize the neutron streaming into the upper plenum while providing sufficient void spacing for passage of the coolant gas. Many of the design problems in the exit shield were similar to those studied for the Grid Plate Shield concept and, as a result of that work, were not approached in this experiment. There was, however, a concern about the validity of the calculation of the neutron streaming through the exit shield with the presence of a control rod in the fuel-pin array and blanket. Therefore, a study of these effects was made. An analysis of this experiment will follow in a separate report which will contain comparisons between measurements and calculations with descriptions of the calculational methods used.

The experimental configuration consisted of four basic segments: a concrete shadow shield placed directly in the collimated neutron beam from the Tower Shielding Reactor (TSR-II); a simulated GCFR core directly behind the shadow shield; a cross section of a prototypic exit shield without the control rod; and a cross section of a prototypic exit shield with a control rod. Part of the simulated core (fuel pins) was considered to be representative of the axial blanket during these measurements.

A pitch of 1.8 cm was selected for the fuel pin spacing, resulting in 91 pins per subassembly. The exit shield subassemblies were scaled to be prototypic of those designed for the 300 MW(e) reactor. The spacing between the subassemblies was selected to be .635 cm. The control rod was divided into two equal segments so that a study of the neutron streaming through the exit shield could be made for several positions of the control rod within 1) the core, 2) the core and axial blanket and 3) the blanket and exit shield. Measurements were made for these locations of the control rod with and without B_4C in the subassembly liner.

Integral and spectral neutron measurements were made using Bonner balls, Hornyak button, NE-213 spectrometer, and hydrogen-filled proton recoil spectrometer. The spectral measurements behind the exit shield were made to provide a neutron source term for calculation of the neutron streaming through the upper plenum and plenum shield.

INSTRUMENTATION

A Bonner ball detector measures an integral of the neutron energy flux weighted by the energy-dependent response function for that ball. The detection device of the Bonner ball consists of a 5.1-cm spherical proportional counter filled with approximately one-half atmosphere of $^{10}BF_3$. This proportional counter is used bare, cadmium covered, or enclosed in various thicknesses of polyethylene shells surrounded by cadmium. Bonner ball experimental results are predicted analytically by folding a calculated neutron spectrum with the Bonner ball response functions calculated by Maerker et al.[2] and C. E. Burgart et al.[3]

Neutron spectral measurements were obtained in the region from about 800 keV to 15 MeV using a NE-213 liquid scintillator and from about 50 keV to 1 MeV using spherical proton recoil counters filled with hydrogen to pressures of 1, 3, and 10 atmospheres. The NE-213 neutron pulse-height data were unfolded using the FERD code to yield absolute neutron spectra. Pulse-height data from the hydrogen-filled counters were unfolded using SPEC-4, with the unfolded NE-213 neutron spectrum used for the high-energy input spectrum.

The Hornyak button has a response to neutrons that closely approaches that of a fast neutron dosimeter.[4] For this experiment the button was 0.635 cm in diameter, 0.159-cm thick, and mounted on an RCA photomultiplier tube. The calibration procedure consisted of first exposing the scintillator to a 2 R/h gamma-ray dose rate and the electronic gain adjusted to obtain a prescribed count rate for a pulse height setting of six-tenths volt (PHS=060). The button was then exposed to a known intensity ^{252}Cf neutron source and a count rate obtained for a PHS of 300. Calibration at this higher PHS (rather than 060) was necessary to bias above the maximum pulse height reached from gamma-ray induced pulses during the measurements behind the configuration. Calibrations and measurements were obtained at this PHS even though for some of the measurements the magnitude of the gamma flux was considerably less.

The measurements for each detector used in the experiment are referenced to the reactor power during the run using two fission chambers that were previously normalized to an established reactor power. The fission chambers, through the use of iron inserts, are capable of providing a measurement of the reactor power over the range from 0.1 W to 1 MW.

3. EXPERIMENTAL CONFIGURATION

3.1 Concrete Shadow Shield and Surrounding Reflector

One of the requirements for this experiment was a source of neutrons whose spectrum was very similar to that expected to be axially streaming from the GCFR core. To do this, it was necessary to minimize the neutron contribution at the exit shield from the TSR-II reactor with respect to the flux whose origin lies within the fuel pins simulated core. Calculations made for a previous experiment[4] indicated that 90% of the source term would lie within the fuel pins by placing a concrete shadow shield 76.2 cm in diameter and 30.5-cm thick, with a surrounding void, between them and the TSR-II (Fig. 1). The circumference and the

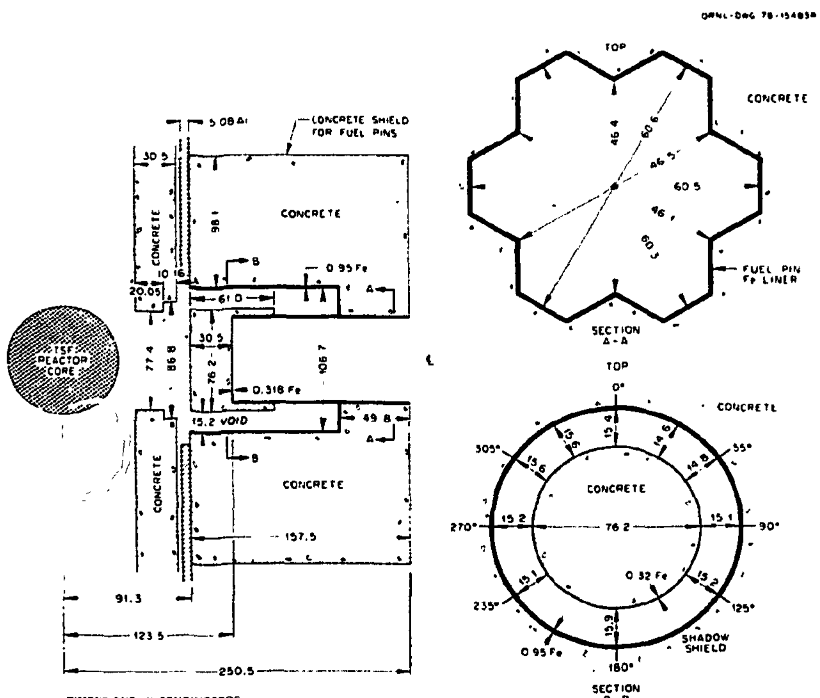

Fig. 1. A schematic of the concrete slab surrounding the fuel pin subassemblies.

face of the shadow shield away from the reactor were covered with a 0.318-cm thickness of iron (Fe) that was attached to the Fe forming the fuel pin cavity. The 15.2-cm void region around the shadow shield was designed to maximize the flux generated within the fuel pins. This region was extended along the initial 61 cm of the fuel region after which the remaining length of the void (45.7 cm) widened to the Fe liner that formed the cavity for the fuel pin region. The outside of this 15.2-cm void was lined with 0.95-cm Fe. All of this was contained in a 157.5-cm-thick concrete slab that was 305-cm wide and 213-cm high. The composition of the concrete slab and shadow shield is given in Table 1.

3.2 GCFR Simulated Core

The GCFR core was simulated by seven subassemblies containing slightly enriched UO_2 fuel pins (1.99% ^{235}U) clad in 0.815 mm wall aluminum tubing having an OD of 1.27 cm (see Fig. 2).

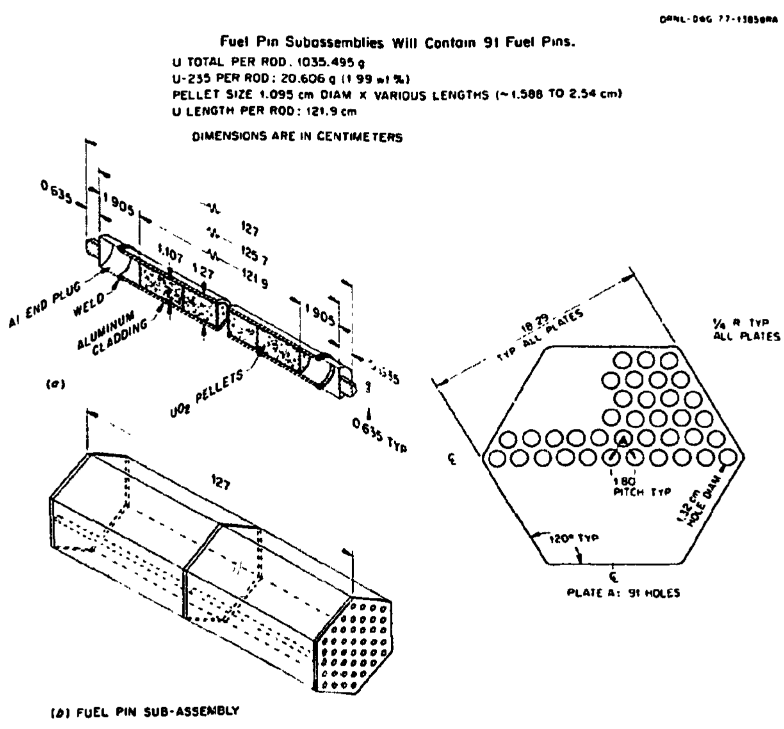

Fig. 2. Schematic of fuel pin and fuel pin subassembly.

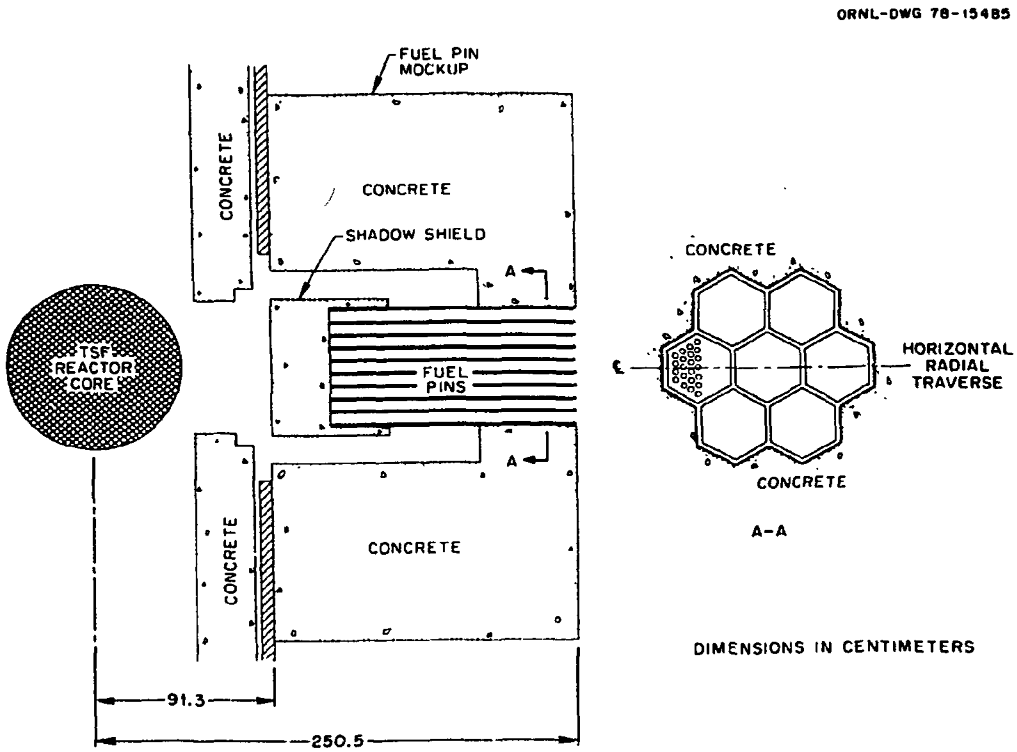

Fig. 3. The initial mockup of shadow shield and fuel pin subassemblies. *(Item I-A)*.

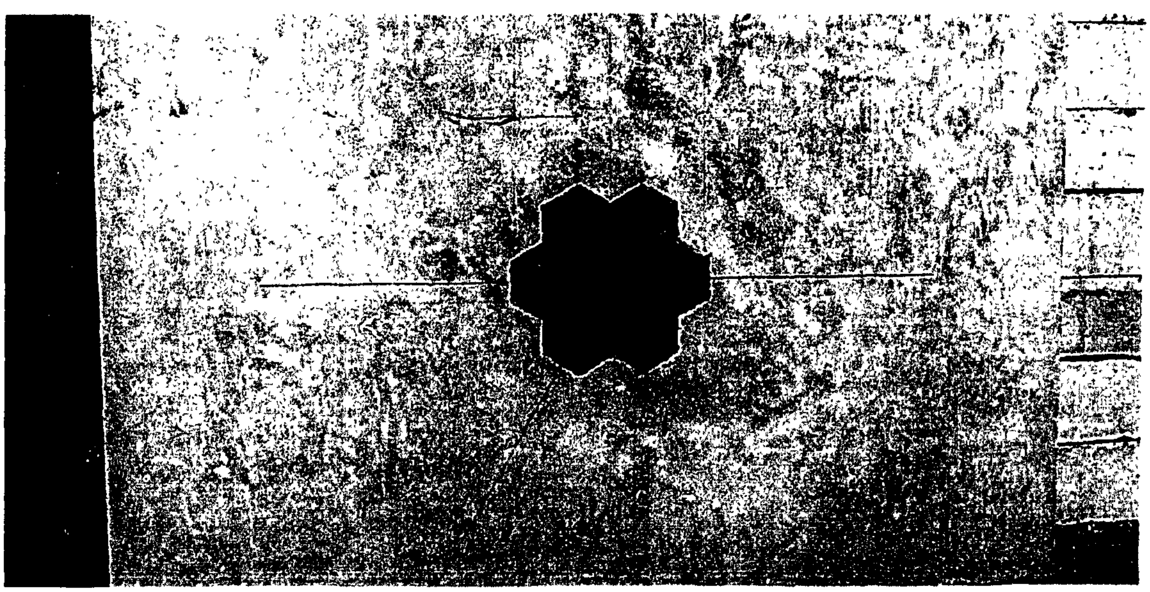

Fig. 4. Mockup of fuel pin subassemblies *(Item I-A)*.

Each pin contained approximately 1035 g of U in the form of small pellets placed end on to give a length of 121.9 cm. Aluminum studs were placed on each end, giving an overall rod length of 127 cm.

The subassemblies were hexagonal in shape and the walls were fabricated from 0.30-cm-thick carbon steel. The design of the subassemblies called for 18.3 cm between opposite flat surfaces. Each subassembly was 127-cm long and contained 0.318-cm-thick support grids, one in the middle and one at each end to maintain proper pitch between the pins. Seven subassemblies modeled the core with each subassembly containing 91 pins with a pin pitch of 1.80 cm (Fig. 3). A semi-quantitative analysis of the impurities in the Fe is given in Table 2.

Spacing between subassemblies was maintained at 0.635 cm (±5%) throughout the experiment. This was accomplished through the use of a series of small steel pieces placed near the ends of the flat surfaces on the subassemblies and at the middle. A picture of the mockup is given in Fig. 4.

3.3 Exit Shield

The dimensions of the exit shield subassemblies as designed for the GCFR 300 Mw(e) reactor were somewhat larger than the subassemblies containing fuel pins used in a prior experiment at TSF. Calculations indicated that about 77% reduction in volume was necessary to fabricate assemblies to correspond with the dimensions of the fuel pin subassemblies. This factor was applied to the volume of B_4C and the void spacing but the iron wall thicknesses were selected on the basis of material availability, namely, the same as for the fuel pin subassemblies.

The outer liners of the exit shield subassemblies were hexagonal in shape matching those of the fuel pin subassemblies (see Fig. 5). The inner liners were cylindrical, with one portion of it tapered along the axis, reducing the peripheral shield thickness from about 5.9 cm to about 2.8 cm over 36.5 cm of the subassembly after which it remained at 2.8 cm. This thickness was defined by pieces of Fe as shown at each end of the subassembly. The void between the liners was vibra-packed with B_4C to densities varying from about 1.34 to 1.37 g/cc for the seven subassemblies (see Table 3). The overall length of the B_4C portion of the subassembly was 76.2 cm, when added to the Fe end pieces gave an overall length of 83.5 cm.

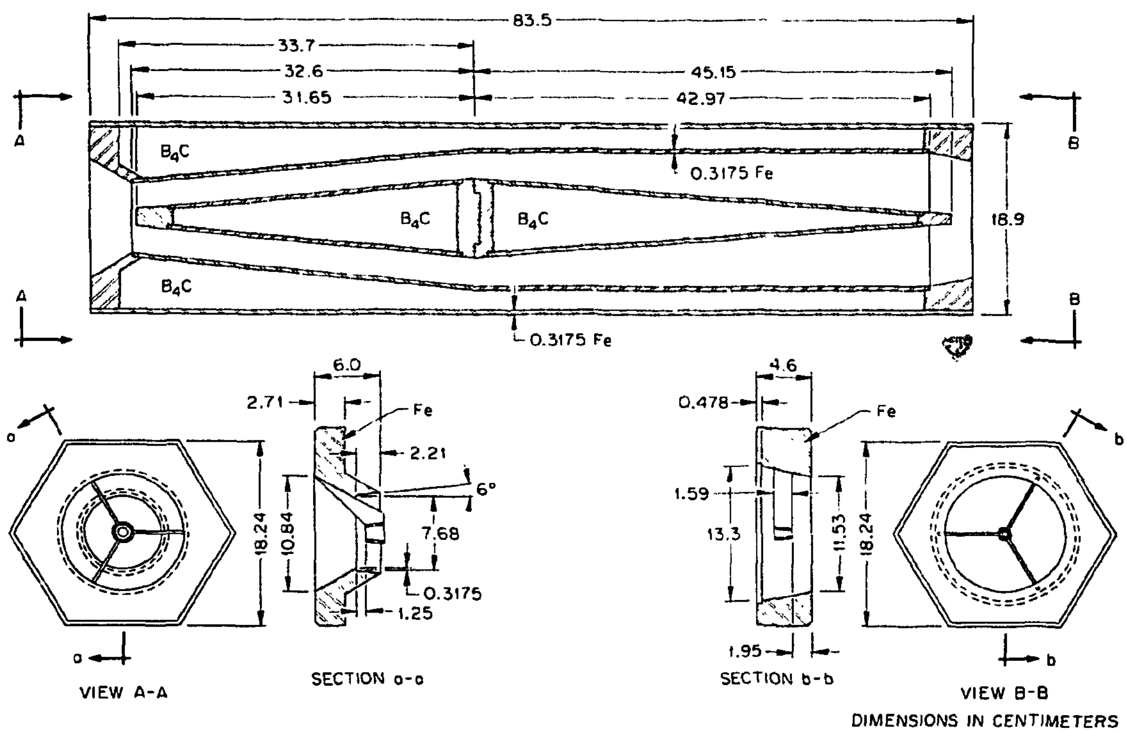

Fig. 5. Schematic of exit shield subassembly.

Centered on the axis of each subassembly were two cones of unequal length filled with B_4C and joined at the large ends of the cones. The taper of the shortest cone corresponded to that of the tapered liner of the subassembly, while the longer cone went from a diameter of 7.92 cm to a diameter of 1.43 cm over a length of 42.52 cm (see Fig. 6). The cones were supported within the subassembly by thin Fe fins attached to the Fe end pieces of the subassemblies. The density and analysis of the B_4C in both the cones and subassemblies are listed in Tables 3 and 4. These subassemblies were enclosed in a 0.95-cm Fe liner surrounded by a slab of concrete 83.5-cm thick, 305-cm wide, and 213-cm high (Fig.7). The analysis of the concrete is given in Table 1.

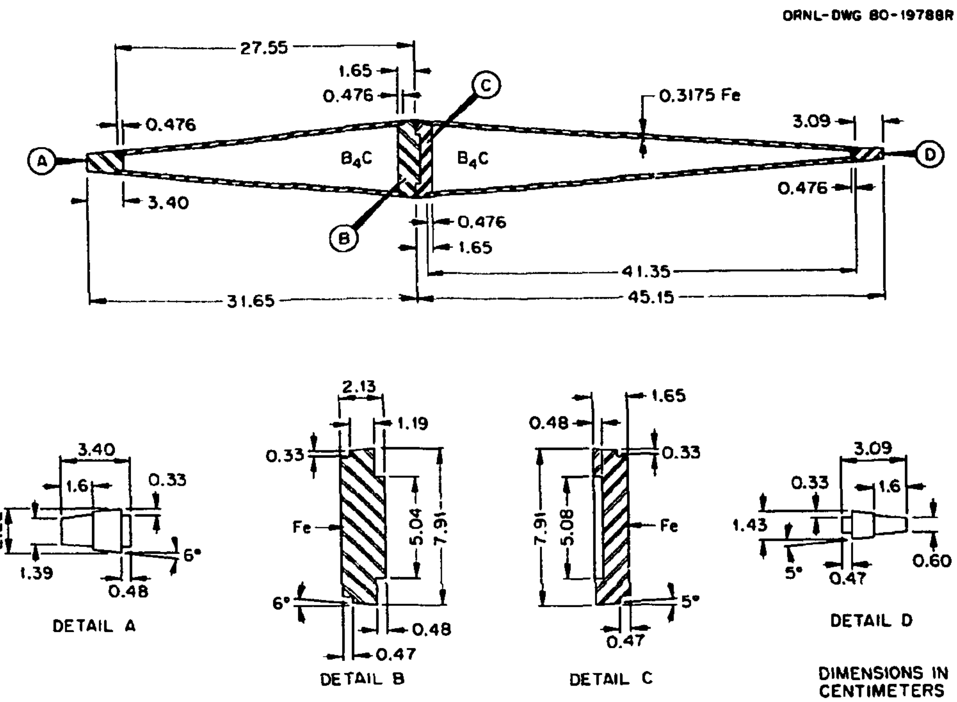

Fig. 6. Schematic of B_4C cones in exit shield subassembly.

3.4 Control Rod and Subassembly

The control rod subassembly consisted of two individual sections; a short piece, 82-cm long, extending from the concrete shadow shield through part of the fuel pin configuration, followed by a longer piece that extended through the exit shield. In the short section the space between the cylindrical inner liner and the hexagon shaped outer surface was left void (Fig. 8). Two pieces of the longer section (128.5 cm) were fabricated, one with a void between the inner and outer liners and the other with this void filled with B_4C. The outer shells of the three subassemblies matched the other subassemblies and the inner liners were 16.14 cm in diameter (ID).

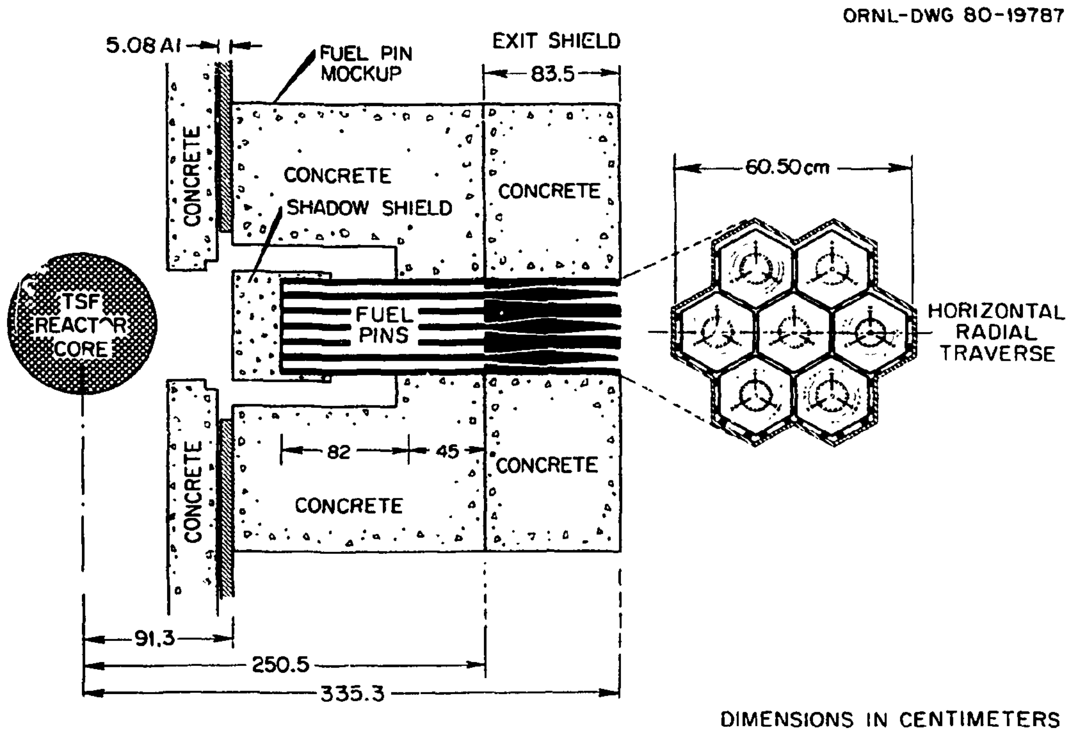

Fig. 7. Second configuration, which includes addition of seven hexagonal exit shield subassemblies *(Item II)*

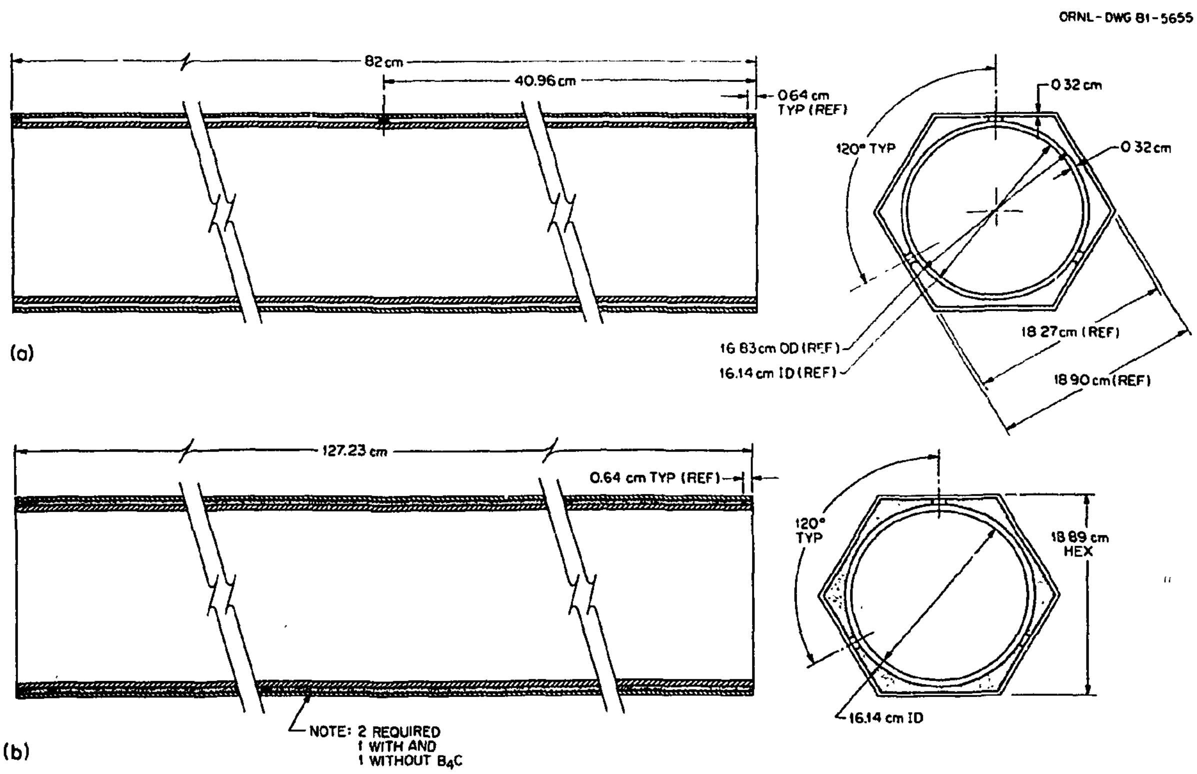

ı]. 8. Schematic of the control rod sleeves *(Items III, IV)*

This separation was designed into the experiment since the first 82 cm was to remain void (subassembly shell only) throughout the remainder of the experiment. This helped minimize the loss of run time as well as cutting labor costs by permitting the second sections (the longer lengths with and without B_4C between liners) to be exchanged from behind the exit shield without the tedious task of removing the concrete slab containing the exit shield a second time, exchanging the central subassembly in the fuel pin mockup, and then putting the exit shield back into its original position.

The spacings between subassemblies in the exit shield for mockups with and without the control rod subassembly were kept the same, with the voids averaging slightly more than the designed .635 cm by several percent as seen in Fig. 9. As a result of this small spacing between subassemblies there was a much larger void, as much as 1.25 cm, between subassemblies and the iron-liner in the concrete shield. A photo of the exit shield is shown in Fig. 10.

ORNL-DWG 80-19789

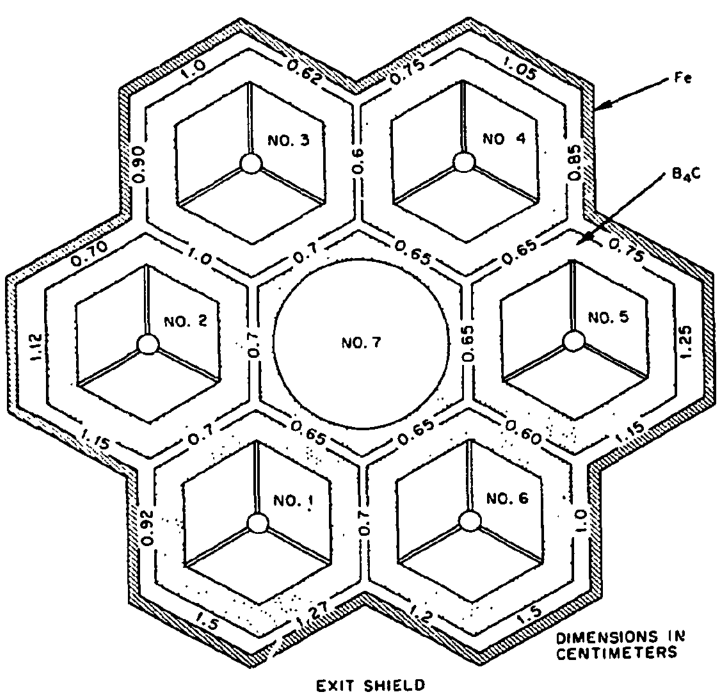

Fig. 9. Schematic of void spacings measured between exit shield subassemblies.

ORNL PHOTO 81-9550

Fig. 10. Mockup of exit shield with control rod sleeve *(Items III, IV)*

The cylindrical control rod was fabricated into two sections, each 60-cm long and 15.9-cm OD (see Fig.11). Both sections were filled with B_4C. The control rod follower was also fabricated into two sections so that for each of the three positions of the control rod within the mockup, the follower would not extend beyond the exit shield and interfere with measurements. Each section of the follower was filled with B_4C. Analysis and densities of the B_4C in the control rod and its follower are listed in Tables 4 and 5 respectively.

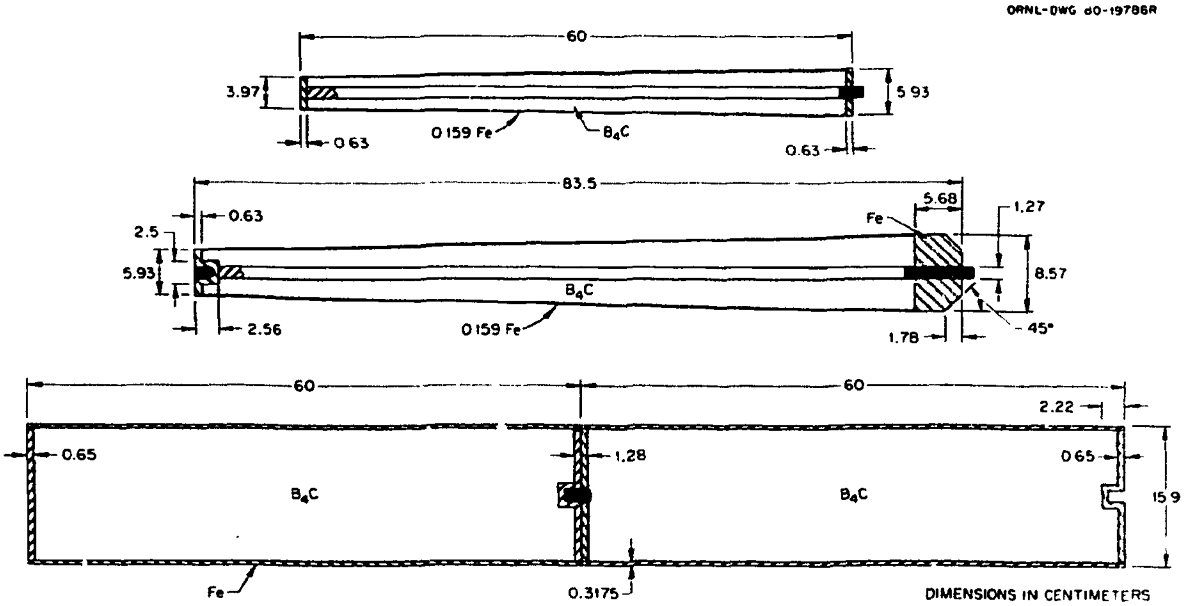

Fig. 11. Schematic of control rod and control rod follower.

4. MEASUREMENTS

4.1 Fuel Pin

For the initial configuration, a slab of concrete containing seven subassemblies of 91 fuel pins each was placed in the reactor beam (Fig. 3). Since this mockup had been thoroughly studied and the results previously presented [5], a minimum number of measurements were required behind the fuel pins to reassure ourselves that the magnitude and spectra of the neutron flux were well known.

Horizontal traverses with the Hornyak button, 2- and 5-in. diam Bonner balls were made at 30.5 cm behind the fuel pins and these results are listed in Table 6 and plotted in Fig. 12. The neutron spectrum measurement at 155.4 cm behind the fuel pins obtained with the NE-213 scintillator is plotted in Fig. 13 and listed in Table 7. The low energy part of the spectrum obtained with the proton recoil hydrogen-filled detectors at the same location is plotted in Fig. 14 and listed in Table 8. The 2-, 5-, and 10-in. diam Bonner ball measurements at the NE-213 location are given in Table 9.

4.2 Exit Shield

The exit shield was then placed behind the fuel pins, the shield consisting of seven subassemblies also spaced 0.635 cm apart and surrounded by concrete. Care was exercised in aligning the subassemblies with the fuel pin subassemblies so that the streaming path between subassembly walls did not appear to be interrupted. A plan view of the mockup is shown in Fig. 7. Spectral measurements with the NE-213 and hydrogen-filled proton recoil counters were made on centerline at 39.8 cm behind the exit shield. These spectra are plotted in Figs.15 and 16 and listed in Tables 10 and 11 for the NE-213 and hydrogen counters respectively. Measurements with 2-, 5-, and 10-in. Bonner balls along with the Hornyak button were also made on centerline at the 39.8-cm location and these results are given in Table 9. The radial traverse at 1.9 cm

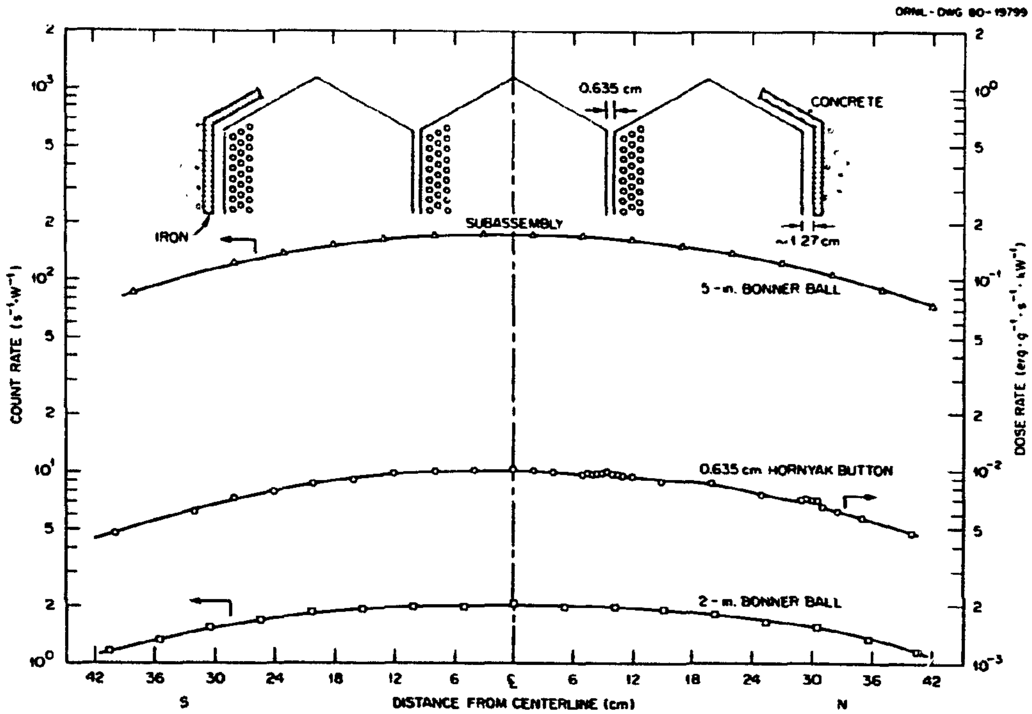

Fig. 12. Radial traverses at 30.5 cm behind fuel pins with Hornyak button and Bonner balls. *(Item I-A)*.

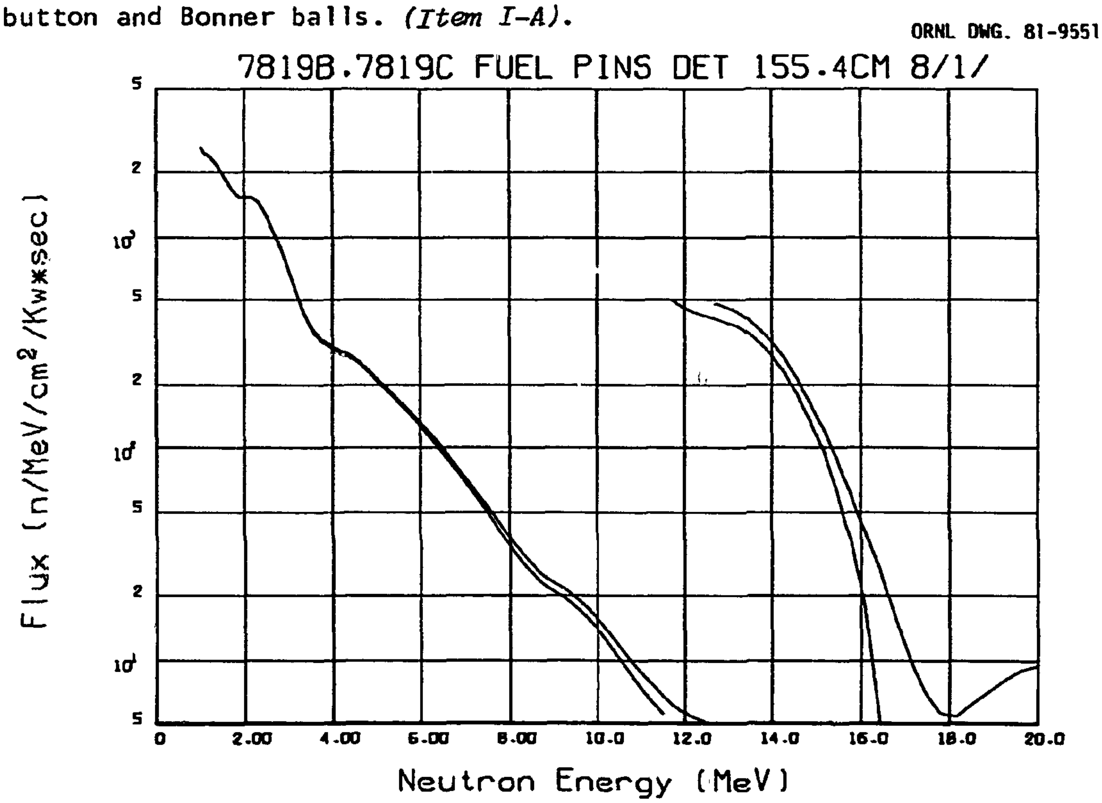

Fig. 13. High energy neutron spectrum on centerline at 155.4 cm beyond fuel pins *(Items I-A)*.

ORNL DWG. 81-9552

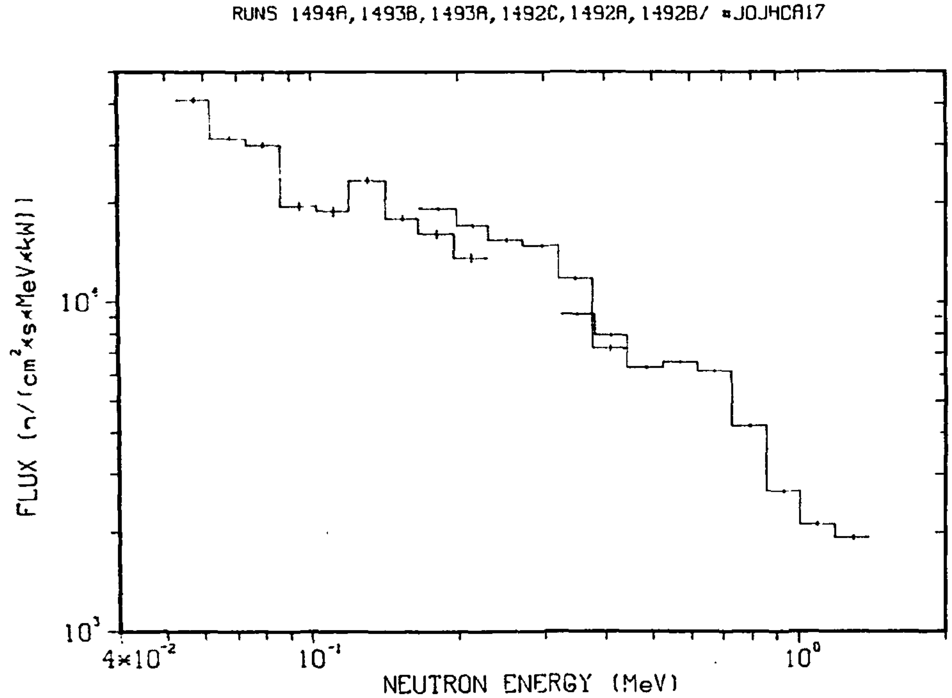

Fig. 14. Neutron spectrum from 100 keV to 1.4 MeV on centerline at 155.4 cm beyond fuel pins *(Item I-A)*.

ORNL DWG. 81-9553

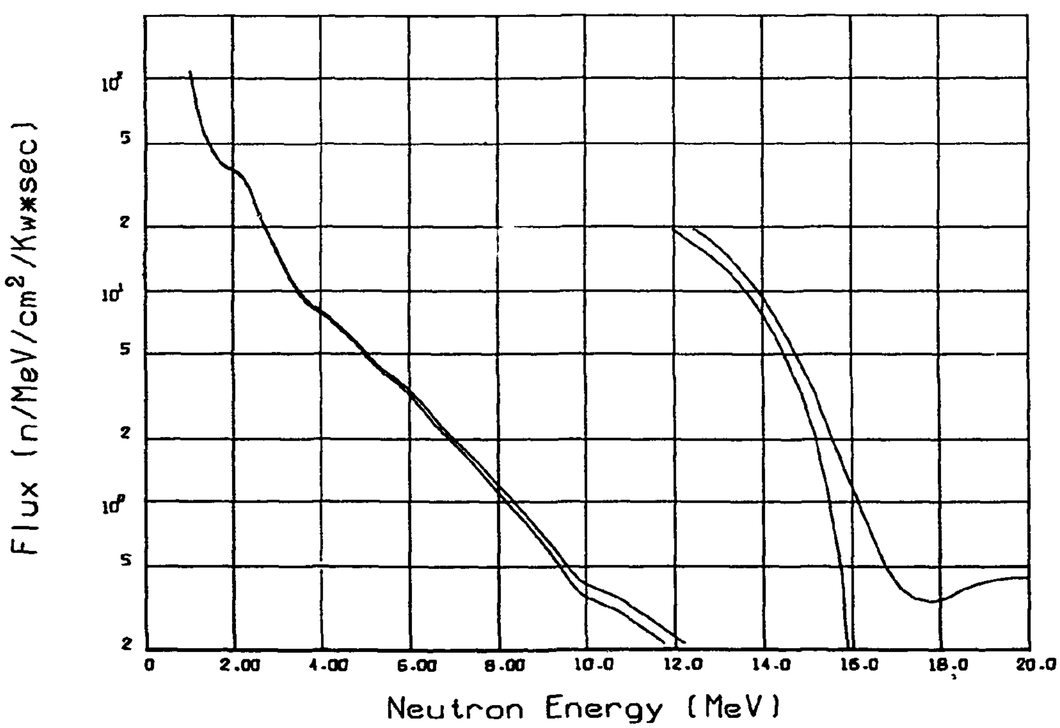

Fig. 15. High energy neutron spectrum on centerline at 39.8 cm beyond fuel pins plus exit shield *(Item II-A)*.

behind the exit shield with the Hornyak button, shown in Fig. 17, along with the 2- and 5-in. Bonner ball data display expected peaks at the voids between subassemblies and between the subassemblies and the concrete shield. It should be noted that in this experiment traverses are always made in the horizontal plane through the reactor beam-shield sample centerline. The relative magnitudes of the peaks at the concrete interface reflect the void spacing at that point and the difference in flux intensities in the fuel pins in each of the areas. The peaks at the subassembly interfaces are nearly the same. Data directly behind the subassemblies gives a good picture of the alignment of the two cones placed within the subassemblies. The peaks behind the subassembly on the right indicate the cones to be centrally located. The cones in the other two subassemblies are slightly off center to the left, allowing a greater number of neutrons to stream through on the right hand side.

ORNL DWG. 81-9554

RUNS 1496A, 1496B, 1497A, 1495B, 1495A/ *JOJHCA18

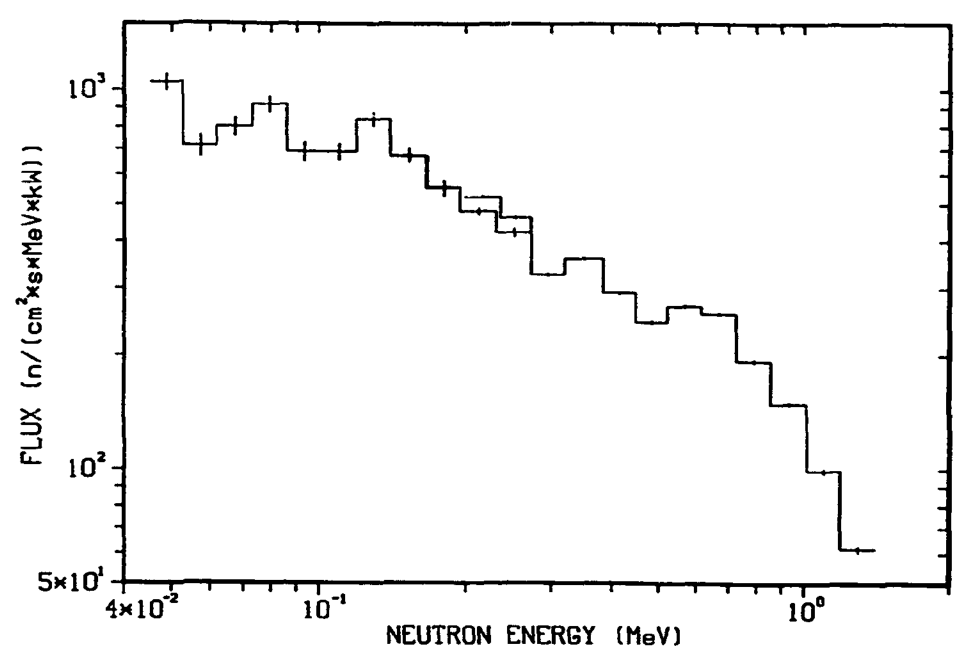

Fig. 16. Neutron spectrum from 100 keV to 1.4 MeV on centerline at 39.8 cm beyond fuel pins plus exit shield *(Item II-A)*.

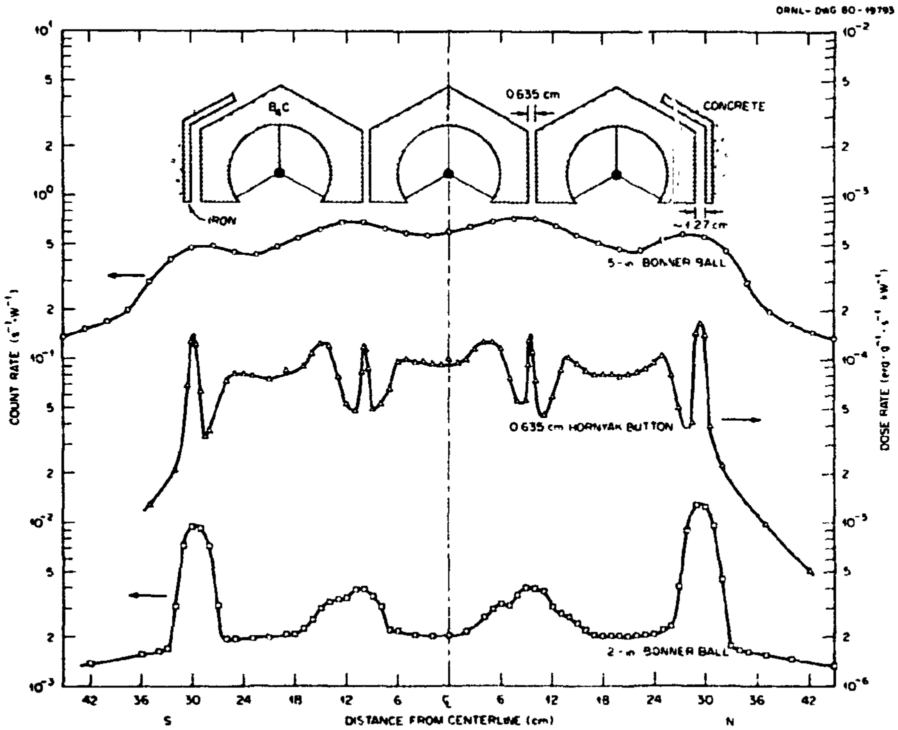

Fig. 17. Radial traverses behind fuel pins plus exit shield with Hornyak button and Bonner balls *(Item II-A)*.

As would be expected, however, due to geometry the streaming through the center subassembly is somewhat greater than for the adjacent ones. The numerical values for the curves in Fig. 17 are given in Table 12.

4.3 Exit Shield with Control Rod Subassembly (no B_4C)

The center subassemblies from both the fuel pins and exit shield were removed and replaced by the control rod subassemblies without B_4C in the void between inner and outer liners (see Fig. 18). The first series of traverses were along the axis of the control rod subassembly without the control rod present. The flux distribution was mapped using both the Hornyak button and the 2-in. Bonner ball. These results are given in Table 13 and plotted in Fig. 19. The slopes of the two curves are essentially the same over the first 100 cm but as they approach the exit shield the slope of the curve for the 2-in. Bonner ball data drops faster than for the Hornyak

ORNL-DWG 80-19781

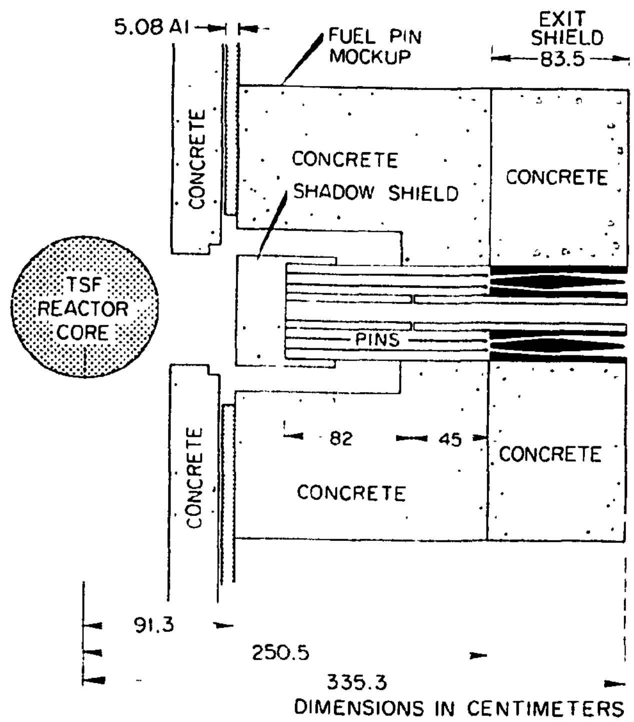

Fig. 18. Schematic of fuel pins and exit shield with central control rod subassembly without B_4C in sleeve *(Item III-A)*.

button, where upon entering the exit shield the two curves once again have essentially the same slope. A radial traverse, made at 1.9 cm behind the exit shield with the Hornyak button, is plotted in Fig. 20 and listed in Table 14. The distribution is flat across the control rod void, dropping sharply at the edge of the exit shield subassembly. Behind the exit shield subassembly the flux decreased slowly until the detector reached the end of the exit shield where the flux dropped sharply only to peak again at the outer void. Radial traverses were made at 39.8 cm behind this configuration with the 2-in. and 5-in. Bonner balls and the data are plotted in Figs. 21 and 22 and listed in Table 15 and 16 respectively. These measurements were complemented with centerline

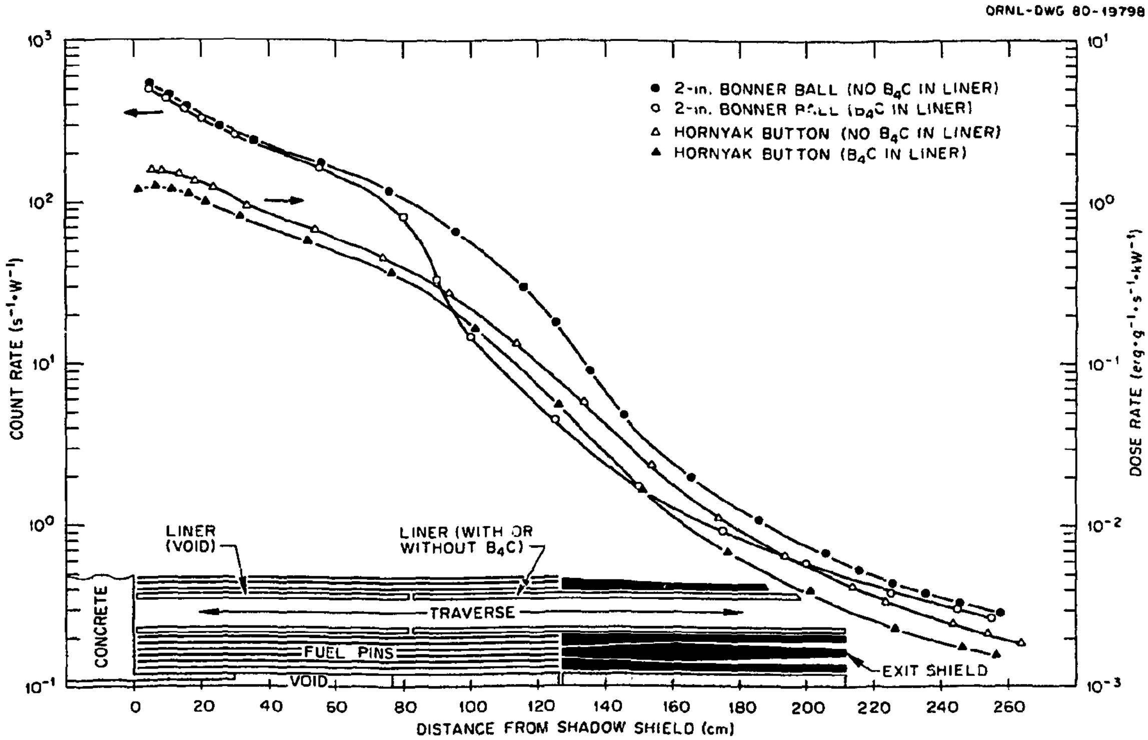

Fig. 19. Axial traverses through fuel pins and exit shield with 2-in. Bonner ball and Hornyak button, no B_4C in control rod sleeve *(Item III-A)*.

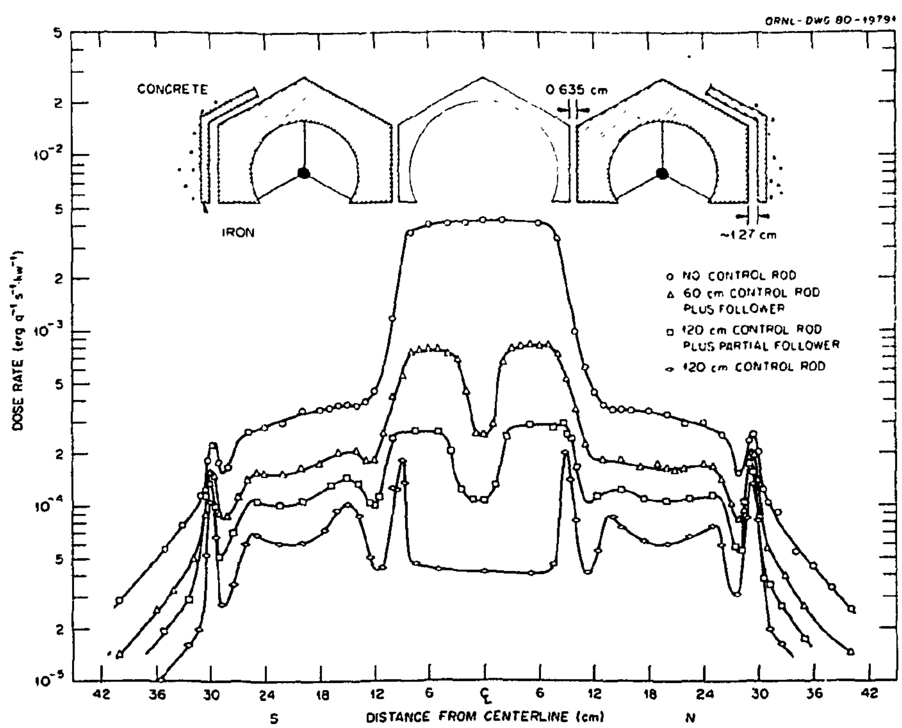

Fig. 20. Radial traverses at 1.9 cm behind fuel pins plus exit shield with Hornyak button for several control rod positions, no B_4C in control rod sleeve *(Items III-A, III-B, III-C, III-D)*.

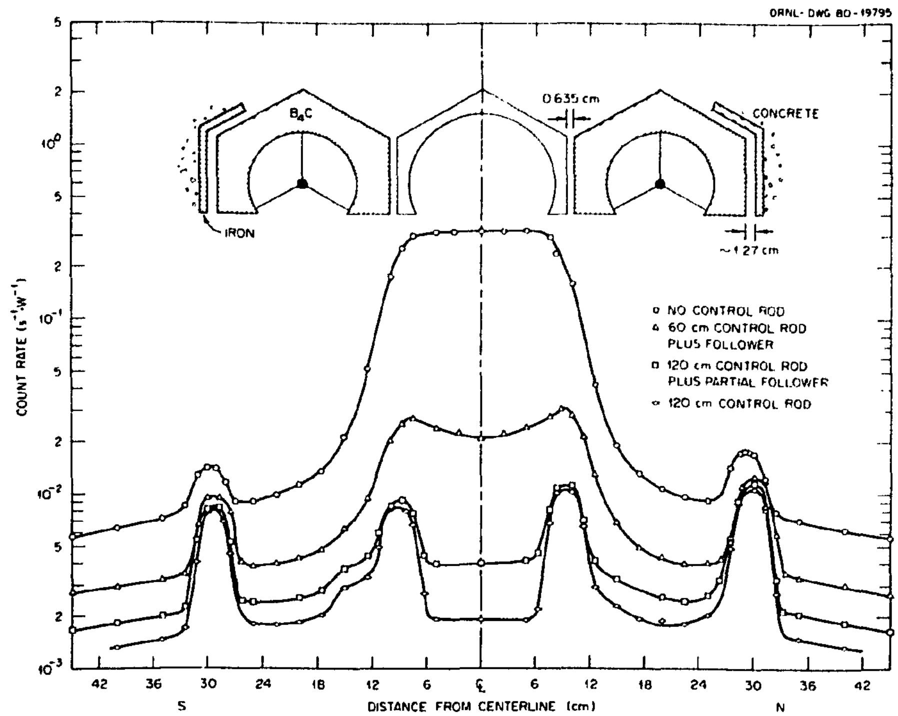

Fig. 21. Radial traverses at 39.8 cm behind fuel pins plus exit shield with 2-in. Bonner ball for several control rod positions, no B_4C in control rod sleeve *(Items III-A, III-B, III-C, III-D)*.

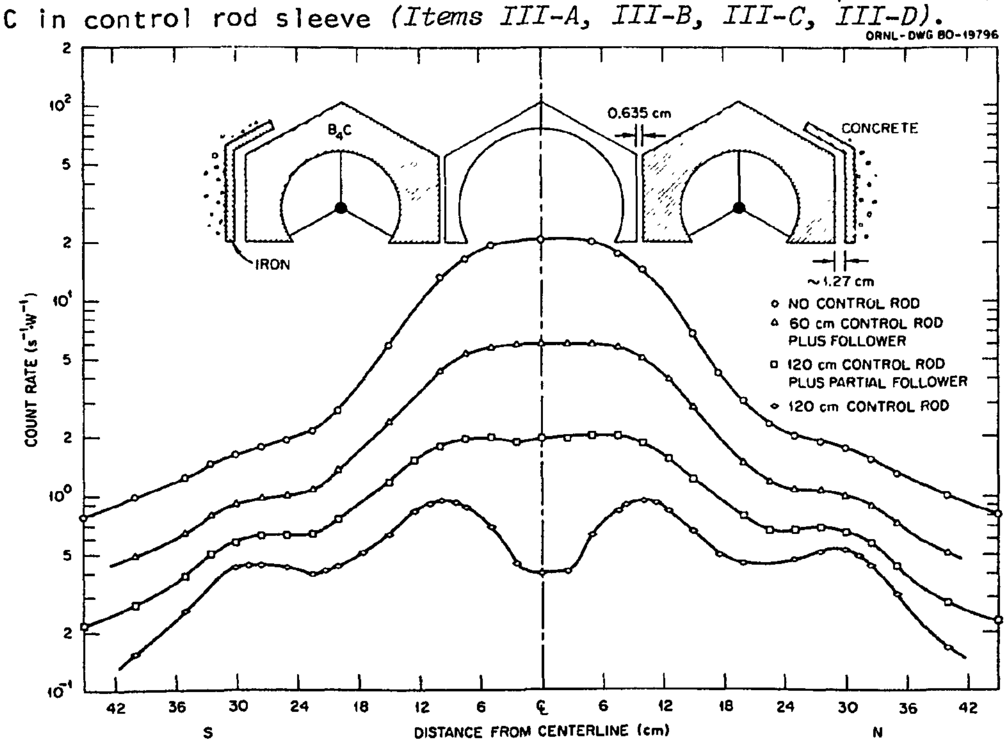

Fig. 22. Radial traverses at 39.8 cm behind fuel pins plus exit shield with 5-in. Bonner ball for several control rod positions, no B_4C in control rod sleeve *(Items III-A, III-B, III-C, III-D)*.

measurements also at 39.8 cm using the Hornyak button and 10-in. Bonner ball. The data are given in Table 9. It should be noted that throughout the presentation of the data in this report no corrections in the detector location with respect to the centerline have been made even though locations of the peaks may indicate small errors in the original positioning of the detector.

The next series of measurements were for three positions of the control rod within the control rod subassembly. In the first position one half of the control rod (60 cm) plus the control rod follower were placed in the control rod cavity such that the end of the control rod was 7 cm from the concrete shadow shield. For this position the end of the control rod follower was coincident with the back face (face away from the reactor) of the exit shield (Fig. 23). An additional 60 cm of control rod was then added to the first 60 cm (now 120 cm total) and positioned again so that the end

ORNL-DWG 80-10678R

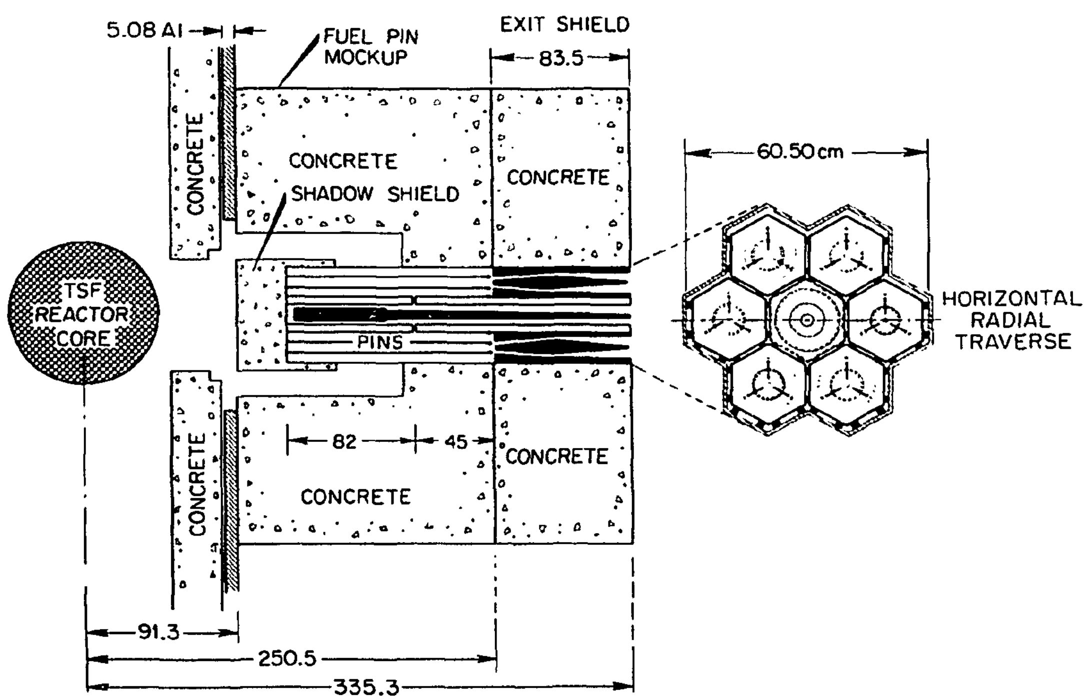

Fig. 23. Schematic of fuel pins and exit shield with central control rod subassembly without B_4C in sleeve, control rod fully inserted *(Item III-B)*.

of it was 7 cm from concrete shadow shield. Adding the 60 cm of control rod necessitated the removing of the small cone section from the control rod follower to keep the end of the follower at the face of the exit shield (see Fig. 24). This position mocks up a partial withdrawal of the control rod from the core into the blanket region. The third and last location of the control rod was to simulate its complete withdrawal from the core. For this mockup the control rod was pulled back from the shadow shield until the outer face of the control rod was flush with the back face of the exit shield with the control rod follower completely removed (see Fig. 25).

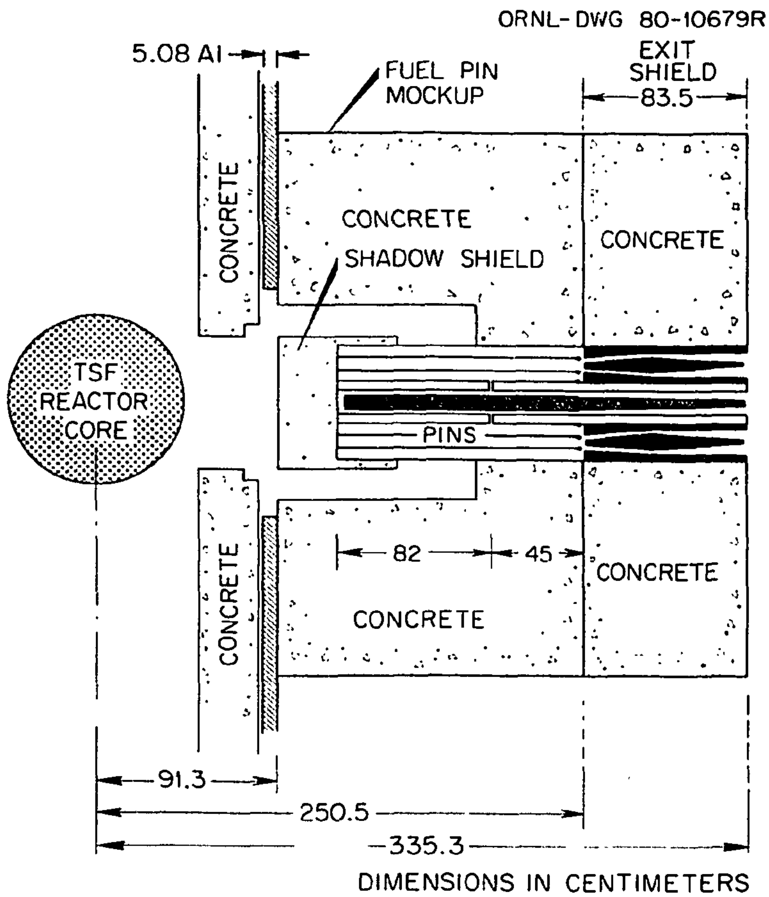

Fig. 24. Schematic of fuel pins plus exit shield with central control rod subassembly without B_4C in sleeve, control rod partially withdrawn *(Item III-C)*.

ORNL-DWG 80-10680R

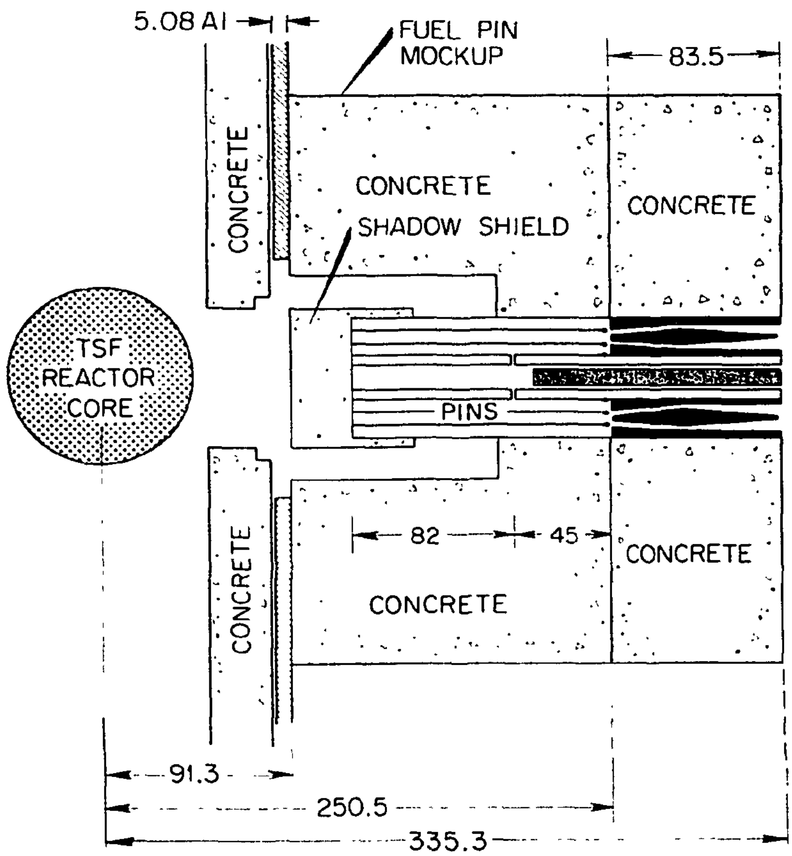

Fig. 25. Schematic of fuel pins plus exit shield with central control rod subassembly without B_4C in sleeve, control rod fully withdrawn *(Item III-D)*.

For each of the above control rod positions radial traverses were made in the horizontal plane with the Hornyak button at 1.9 cm behind the exit shield and with the 2- and 5-in. Bonner balls at 39.8 cm. Data from the traverses behind the four configurations (no control rod mockup included) are plotted on the same graph for a given detector for comparison purposes. The plots for the Hornyak button, 2- and › n. Bonner balls can be seen in Figs. 20, 21, and 22 respectively with the values listed in Tables 14, 15, and 16. With the control rod fully inserted into the core (60-cm control rod plus follower) the peak value of the neutron flux measured with the Hornyak button behind the control rod subassembly is reduced about a factor of five from the data without the control rod, with a dip in the flux at centerline directly behind the control rod handler. The data behind the exit shield subassembly in these same two traverses show the ratio narrows to about a factor of two. With the 120 cm of control rod in the fully withdrawn position (no follower) the neutron flux directly behind the control rod is about a factor of two less than what was measured behind a full complement of exit shield subassemblies earlier in the experiment. From the same traverses the data behind the exit shield subassemblies shows the flux to be reduced only about 30%.

For the 5-in. Bonner ball similar comparisons indicate somewhat the same reduction in flux values but for the 2-in. ball the flux along the centerline was reduced about a factor of 15 in going from the no control rod mockup to the 60-cm control rod configuration. The 120-cm control rod data using the 2-in. ball is very similar to the exit shield data except for the extra streaming in the voids. Measurements with the Hornyak button and 10-in. Bonner ball were also made on centerline at 39.8 cm behind the exit shield and these results are given in Table 9.

4.4 Exit Shield with Control Rod Subassembly (B_4C)

The second section of the control rod sleeve subassembly was then exchanged for a similar section whose void between the inner and outer liners was filled with B_4C (Fig. 26). In the absence of the control rod the axial traverses with the Hornyak button and 2-in. Bonner ball were repeated. These results are listed in Table 13 and plotted in Fig. 19. For the Hornyak button traverse there was only about a 30% decrease in flux over the first 100 cm of travel from that measured without B_4C in the sleeve, with this difference increasing slightly beyond that point. For the 2-in Bonner ball the flux magnitudes are about the same over the first 80 cm, beyond which there is a sudden drop of about a factor of 5 with a return to nearly the same value as for the no B_4C case after passing through the exit shield.

The series of radial traverses with the Hornyak button, 2- and 5-in. Bonner balls were repeated for the four positions of the

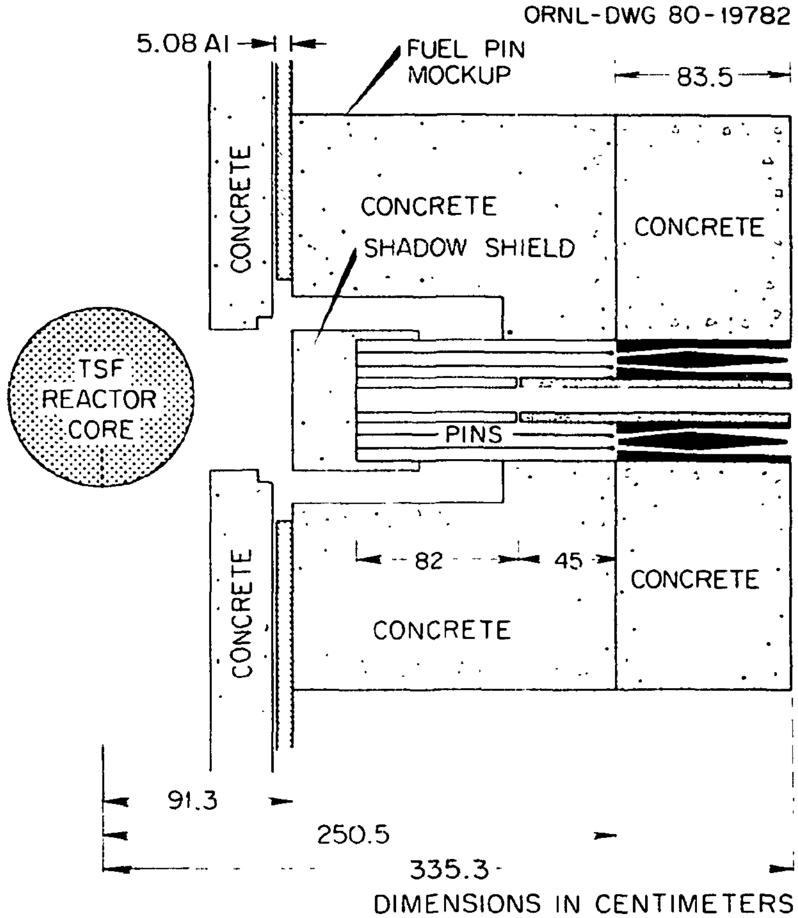

Fig. 26. Schematic of fuel pins plus exit shield with central control rod subassembly with B_4C in sleeve *(Item IV-A)*.

control rod (including no rod) as shown in Figs. 26, 27, 28, and 29. These results are plotted in Figs. 30, 31, and 32 and listed in Tables 17, 18, and 19 for the Hornyak button, 2-, and 5-in. Bonner balls respectively. As expected, the shapes of the curves were essentially the same as in previous series without B_4C in the control rod sleeve except now the streaming effect between subassemblies is more defined as indicated by the appearance of a new peak and valley at about 10 cm off centerline. The presence of the B_4C in the control rod subassembly also reduced the width of the centerline peak with a small effect on its magnitude, maybe 20%. For the 2-in. Bonner ball the magnitude of the centerline peak was unchanged with a very slight reduction in peak width for the no

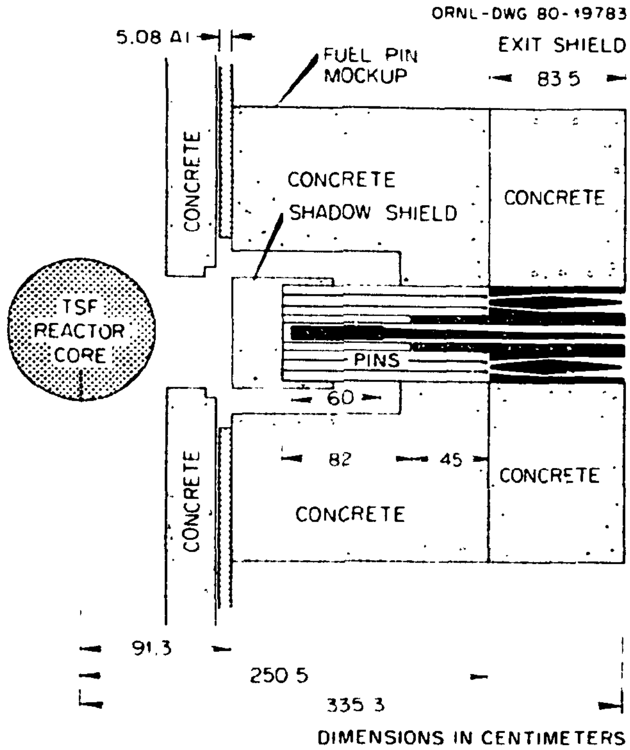

Fig. 27. Schematic of fuel pins and exit shield with central control rod subassembly with B_4C in sleeve, control rod fully inserted *(Item IV-B)*.

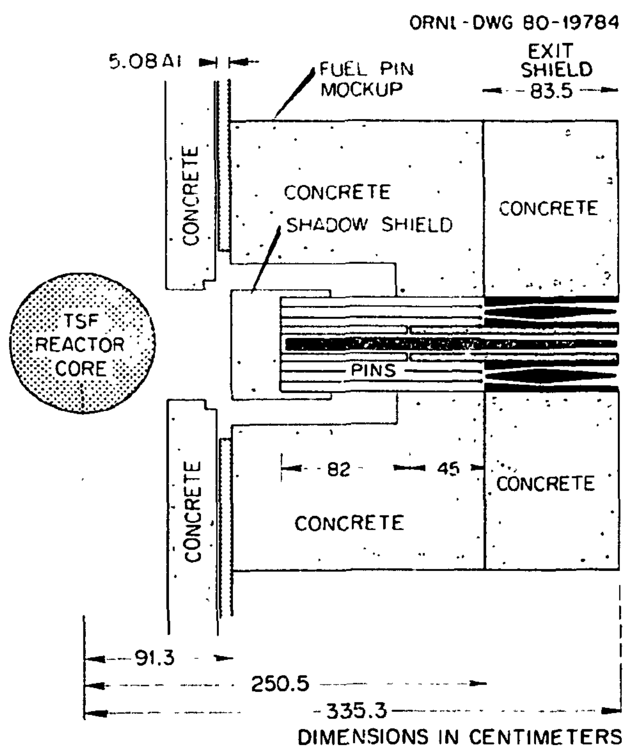

Fig. 28. Schematic of fuel pins and exit shield with central rod subassembly with B_4C in sleeve, control rod partially withdrawn *(Item IV-C)*.

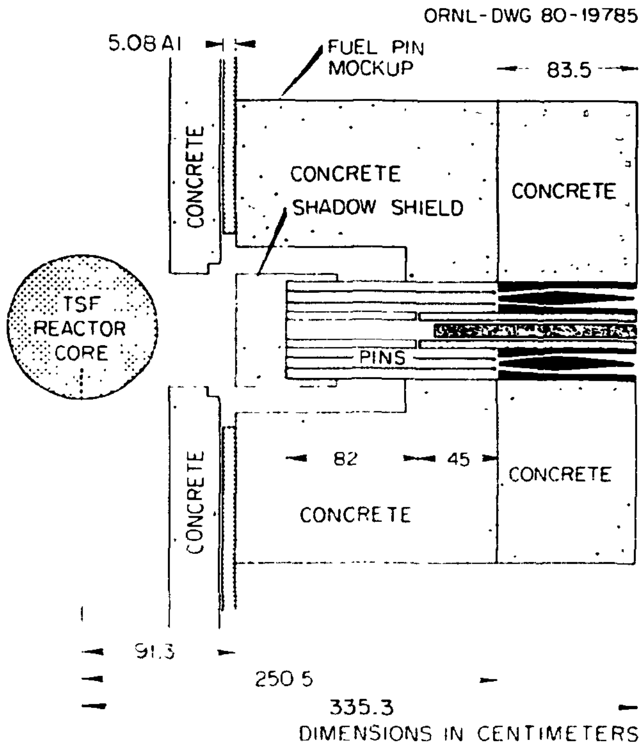

Fig. 29. Schematic of fuel pins and exit shield with central control rod subassembly with B_4C in sleeve, control rod fully withdrawn *(Item IV-D)*.

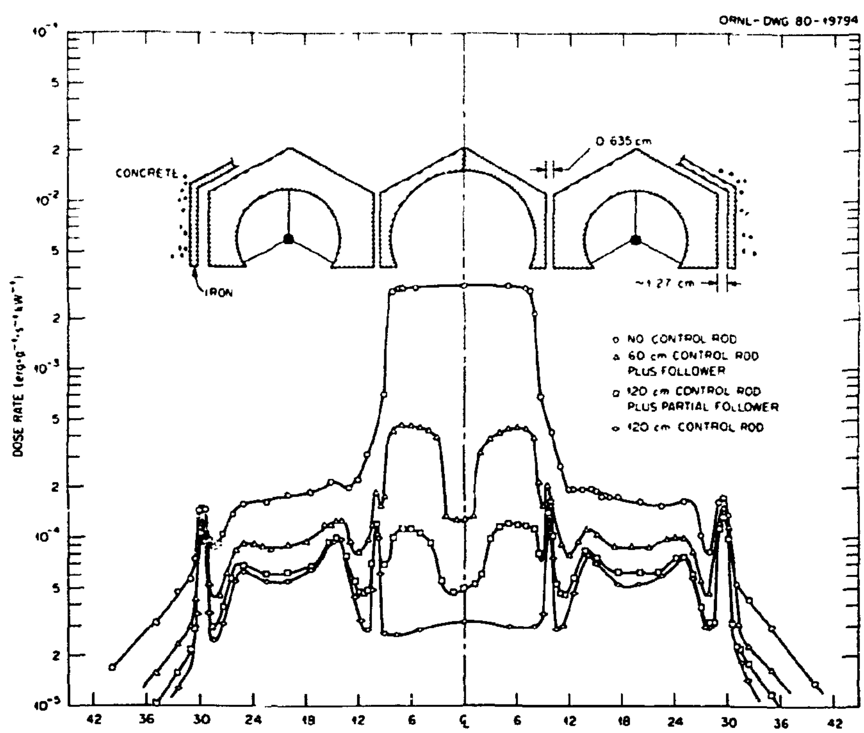

Fig. 30. Radial traverses at 1.9 cm behind fuel pins plus exit shield with Hornyak button for several control rod positions, B_4C in control rod sleeve *(Items IV-A, IV-B, IV-C, IV-D)*.

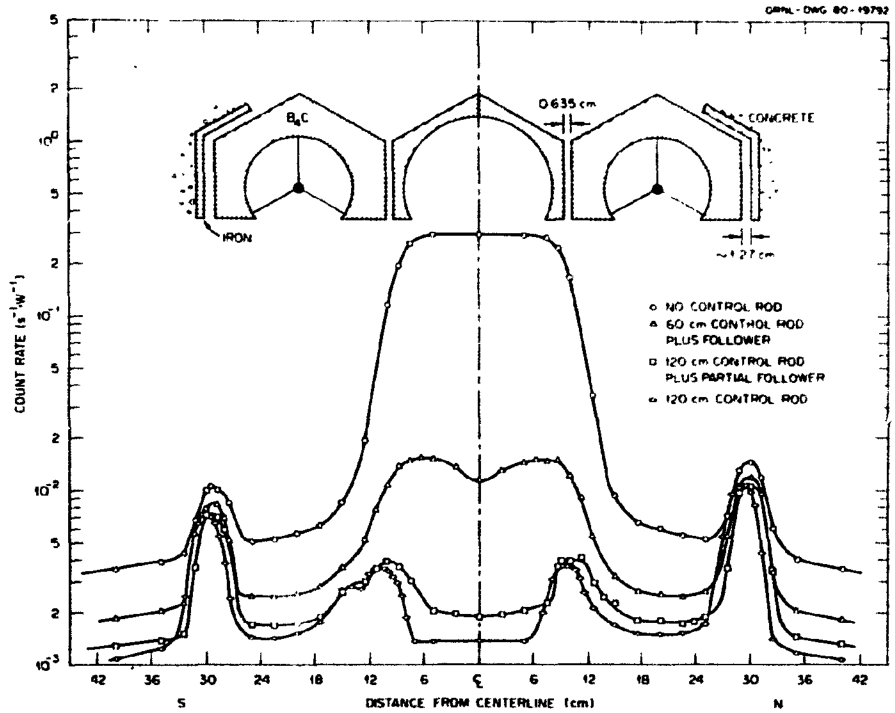

Fig. 31. Radial traverse at 39.8 cm behind fuel pins plus exit shield with 2-in. Bonner ball for several control rod positions, B_4C in control rod sleeve *(Items IV-A, IV-B, IV-C, IV-D)*.

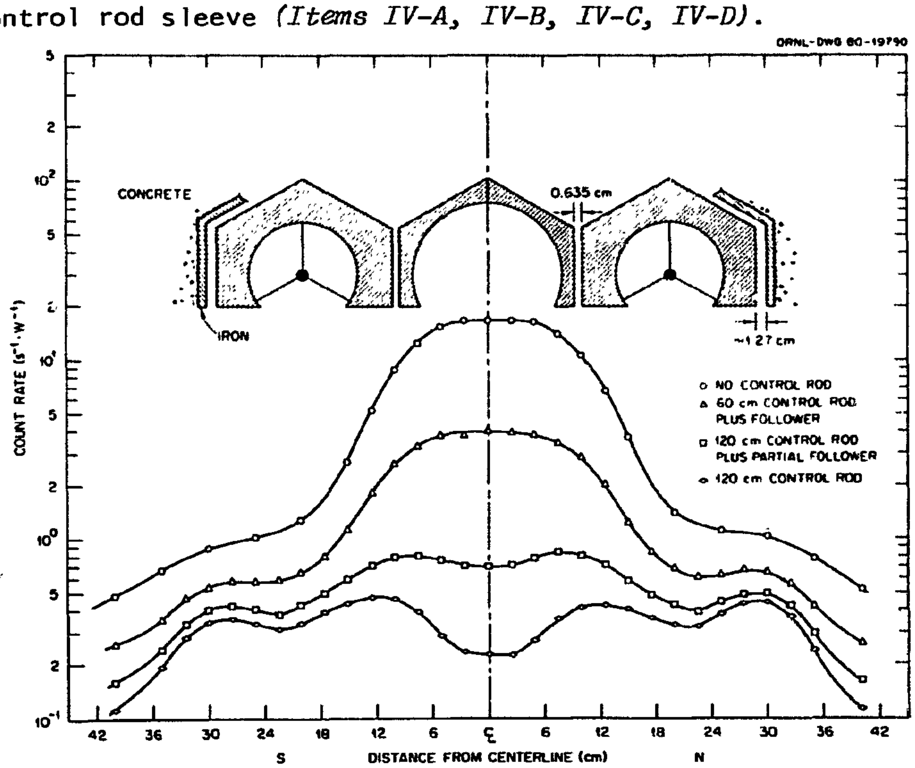

Fig. 32. Radial traverse at 39.8 cm behind fuel pins plus exit shield with 5-in. Bonner ball for several control rod positions, B_4C in control rod sleeve *(Items IV-A, IV-B, IV-C, IV-D)*.

control rod mockup. With the control rod a considerable effect was noticed behind all the subassemblies, not just the control rod. Similar effects were noted for the 5-in. Bonner ball. Centerline measurements with the Hornyak button and 10-in. Bonner ball at 39.8 cm behind the mockups are given in Table 9.

ANALYSIS OF EXPERIMENTAL ERRORS

The error in these measurements normally results from a combination of uncertainties in reactor power determination, detector calibrations, count rate statistics, detector positioning, fabrication tolerances, and the weather. During the measurements the configurations are normally exposed to the weather but for this experiment an attempt was made to limit this effect by covering the mockup with a tarp. Fabrication of components within cost limited budgets requires allowance for larger tolerances than preferred under ideal circumstances. This effect can be seen from the traverses behind the exit shield where peaks and valleys are not symmetrical. No attempt has been made to estimate these effects on the measurements.

A significant source of error in the experiment usually lies in the determination of the reactor power. The power level for each measurement was determined from the outputs of two fission chambers located in the reactor shield along reactor centerline. These detectors were calibrated daily and at one point during the experiment when compared to gold foils placed at the detector locations the non-agreement was less than 5%. During any one detector traverse in a given day the variation in reactor power as indicated by the monitors might be only a few percent. However, over a span of several months of reactor operation the monitors indicated that the power level may have varied as much as 5% from the power level indicated by the reactor control chambers. These variations may indicate the reliability of the monitors or the readings may be a realistic change in the actual power output. Thus, rather than assign an error value to each data point, it would be more realistic to assume, in general, an overall value for the whole experiment of probably less than ±5%.

Count-rate statistics are expressed in a manner exclusive to each detector. For the NE-213, counting statistics and unfolding errors are included in the unscrambling of the pulse-height spectra using the FERD code, with the resultant flux expressed in terms of lower and upper limits that represent a 68% confidence interval. Similar errors are expressed in the tabular data for the hydrogen counter measurements unfolded using SPEC 4. Neither of the spectra, NE-213 or Hydrogen counter, reflects the error in determining the reactor power since this is not fed into the unscrambling. This, as discussed in the previous paragraph, could be as much as 5%.

For the Bonner balls the statistical error in the detector count rates was kept at a maximum of 1-2% by maintaining an adequate count rate. Calibrations over the experimental period indicated about a 3-4% variation. If one now includes the error in reactor power determination for each run, the error in the Bonner ball data would probably average around ±5%.

Data with the Hornyak button probably contains a larger error value than that obtained with the Bonner ball. Despite attempts to maintain temperature stability within the detector systems the wide variations in temperature during a run led to changes in the detector response. It has been estimated from prior experiments that an error of several millimeters in positioning at a distance of 30.5 cm behind the configuration, would result in an error of only 1-2%. Positioning accuracy at distances further from the mockup, of course, would be less stringent. For the Hornyak button closely positioned behind the mockup a strong effort was made to position the detector initially on centerline within a tolerance of 1-2 mm of the 1.9 cm. Since the surface projected by the subassemblies was somewhat irregular the spacing between mockup and detector could not be held within a closer tolerance. Hence, a positioning error of 5% in the data might be suggested for some of the data points. Combining these errors with those from the reactor power determination, calibrations, and counting statistics should give an estimated standard error within $\lesssim$10%.

APPENDIX A

TABLES

Table 1. Analysis of concrete in fuel pin and exit shield slabs

Element	Fuel pin shield concrete (%)	Exit shield concrete (%)
Free H_2O	2.30	1.69
Bound H_2O	4.02	6.04
LOI*	37.62	36.87
SiO_2	11.28	7.9
Fe_2O_3	0.94	0.97
Al_2CO_3	1.30	--
CaO	33.34	43.9
MgO	13.6	7.8
Na_2O	<0.01	<0.1
K_2O	0.50	--
SO_3	0.091	0.86
P_2O_5	0.09	0.05
CO_3	45.9	51.5

*"Lost on ignition"

Table 2. Analysis of Fe used in fabrication of the components listed below

Sample	O	C	Fe
1. B_4C subassembly outer liner	--	519 ppm	99.92%
2. B_4C subassembly inner liner	--	903 ppm	100.26%
3. Fuel pin subassembly liner	24 ppm	484 ppm	99.0%
4. Concrete slab liner	193 ppm	0.21%	97.3%

Semi-quantitative spectrochemical analysis of Fe[a]

	#1[b]	#2	#3	#4
Ag	.05	<.005	<.005	<.005
Al	.05	<.02	.05	<.05
Cr	<.02	<.02	.05	.1
Cu	.01	.01	.02	.05
Fe	M	M	M	M
Mn	.2	.2	.3	.7
Mo	.01	.01	.05	.05
Ni	.02	.05	≤.02	≤.02
Si	.05	.01	.01	.02
V	<.01	<.01	<.02	<.02

[a]wt %
[b]Corresponds to sample number above

Table 3. Weight, volume, and density of B_4C in each component of exit shield subassemblies

Subassembly number	Long cone			Short cone			Subassembly sleeve		
	wt(g)	vol(cc)	den(g/cc)	wt(g)	vol(cc)	den(g/cc)	wt(g)	vol(cc)	den(g/cc)
1	807.2	633.0	1.28	589.6	446.2	1.32	16779.5	12426	1.35
2	820.6	632.6	1.30	570.2	439.2	1.30	16756.8	12471	1.34
3	803.6	626.9	1.28	581.2	445.4	1.31	16892.9	12471	1.36
4	822.3	624.8	1.32	566.8	438.6	1.29	17074.2	12471	1.37
5	810.8	632.8	1.28	578.9	440.0	1.30	16892.9	12403	1.36
6	807.3	631.9	1.28	575.9	438.3	1.31	16961.0	12471	1.36
7	804.0	622.5	1.29	577.3	442.0	1.31	16756.8	12435	1.35

Table 4. Analysis of B_4C used in exit shield subassemblies

	Percentage by Weight	
Grit	Boron	Carbide
120	76.39	22.95

Semi-quantitative spectrochemical analysis of B_4C[a]

Ag	<20	Mg	40
Al	50	Mn	20
B	M	Mo	<25
Ba	<20	Nb	<100
Be	<5	Ni	<10
Bi	<25	Pb	<20
Ca	425	Rb	<100
Cd	<200	Sb	<100
Co	<30	Si	1300
Cr	30	Sn	<25
Cu	200	Sr	<25
Fe	250	Ta	<500
Ga	<20	Ti	100
Ge	<100	V	<25
Hg	<600	W	<200
In	<20	Zn	2700
K	<25	Zr	<100
Li	<10		

[a] ppm

Table 5. Weight, volume, and density of B_4C in the control rod, sleeve, and follower

Component	wt(g)	vol(cc)	den(g/cc)
Control rod sleeve subassembly	11678	8390	1.39
Control rod #1 (first half)	14204	10771	1.32
Control rod #2 (second half)	14149	10725	1.32
Control rod follower (large diameter section)	3855	2954	1.31
Control rod follower (small diameter section)	1210	932	1.30

Table 6. Radial traverses in the horizontal plane at 30.5 cm behind the fuel pins *(Item I-A)*

Distance from centerline (cm)	0.635-cm-diam Hornyak button dose rate (erg/g.s.kW)	Bonner ball count rate ($s^{-1}.W^{-1}$)	
		2-in.-diam	5-in.-diam
82.0 N	--	--	1.53(1)[a]
81.3	--	2.92(-1)	--
80.0	9.44(-4)	--	--
72.0	--	--	2.16(1)
71.1	--	4.25(-1)	--
70.0	1.41(-3)	--	--
62.0	--	--	3.22(1)
61.0	--	6.12(-1)	--
60.0	2.10(-3)	--	--
52.0	--	--	4.88(1)
50.8	--	8.41(-1)	--
50.0	3.14(-3)	--	--
42.0	--	--	7.36(1)
40.6	--	1.14(0)	--
40.0	4.78(-3)	--	--
37.0	--	--	9.01(1)
35.6	--	1.32(0)	--
35.0	5.75(-3)	--	--
32.5	6.19(-3)	--	--
32.0	--	--	1.09(2)
31.0	6.53(-3)	--	--
30.5	7.08(-3)	1.55(0)	--
30.0	7.03(-3)	--	--
29.5	7.28(-3)	--	--
29.0	7.08(-3)	--	--
27.0	--	--	1.24(2)
25.4	--	1.64(0)	--
25.0	7.58(-3)	--	--
22.0	--	--	1.39(2)
20.3	--	1.80(0)	--
20.0	8.69(-3)	--	--
17.0	--	--	1.52(2)
15.2	--	1.90(0)	--
15.0	8.94(-3)	--	--
12.0	9.50(-3)	--	1.66(2)
11.0	9.61(-3)	--	--
10.5	9.75(-3)	--	--
10.2	--	1.97(0)	--
10.0	9.81(-3)	--	--
9.5	9.97(-3)	--	--
9.0	9.81(-3)	--	--
8.5	9.86(-3)	--	--
8.0	9.69(-3)	--	--
7.5	9.81(-3)	--	--
7.0	9.75(-3)	--	1.72(2)
5.1	--	1.97(0)	--
4.0	1.00(-2)	--	--
2.0	--	--	1.73(2)
0	1.03(-2)	2.02(0)	--
3.0 S	--	--	1.75(2)
4.0	1.01(-2)	--	--
5.1	--	1.98(0)	--
8.0	1.01(-2)	--	1.71(2)
10.2	--	1.99(0)	--
12.0	9.69(-3)	--	--

Table 6. (continued)

Distance from centerline (cm)	0.635-cm-diam Hornyak button dose rate (erg/g.s.kW)	Bonner ball count rate ($s^{-1}.W^{-1}$)	
		2-in.-diam	5-in.-diam
13.0	--	--	1.63(2)
15.2	--	1.91(0)	--
16.0	9.06(-3)	--	--
18.0	--	--	1.52(2)
20.0	8.67(-3)	--	--
20.3	--	1.85(0)	--
23.0	--	--	1.38(2)
24.0	7.94(-3)	--	--
25.4	--	1.68(0)	--
28.0	7.28(-3)	--	1.23(2)
30.5	--	1.54(0)	--
32.0	6.17(-3)	--	--
35.6	--	1.32(0)	--
38.0	--	--	8.63(1)
40.0	4.78(-3)	--	--
40.6	--	1.17(0)	--
48.0	--	--	5.82(1)
50.0	3.14(-3)	--	--
50.8	--	8.42(-1)	--
58.0	--	--	3.84(1)
60.0	2.16(-3)	--	--
61.0	--	6.17(-1)	--
68.0	--	--	2.51(1)
70.0	1.41(-3)	--	--
71.1	--	4.39(-1)	--
78.0	--	--	1.78(1)
80.0	9.92(-4)	--	--
81.3	--	3.01(-1)	--
88.0	--	--	1.29(1)

[a]Read: 1.53 X 10^1

Table 7. Run 7819B. NE-213 on centerline at 155.4 cm behind fuel pins *(Item I-A)*

NEUTRON ENERGY (MEV)	FLUX (N/(CM2*S*MEV*KW)) LOWER LIMIT	UPPER LIMIT
8.11E-01	2.07E 03	2.13E 03
9.07E-01	2.69E 03	2.72E 03
1.01E 00	2.61E 03	2.64E 03
1.11E 00	2.44E 03	2.47E 03
1.20E 00	2.38E 03	2.40E 03
1.31E 00	2.26E 03	2.28E 03
1.41E 00	2.09E 03	2.12E 03
1.51E 00	1.94E 03	1.96E 03
1.61E 00	1.80E 03	1.82E 03
1.71E 00	1.66E 03	1.69E 03
1.81E 00	1.56E 03	1.58E 03
1.93E 00	1.51E 03	1.53E 03
2.10E 00	1.52E 03	1.53E 03
2.30E 00	1.46E 03	1.48E 03
2.50E 00	1.26E 03	1.27E 03
2.70E 00	1.00E 03	1.01E 03
2.90E 00	7.80E 02	7.93E 02
3.10E 00	5.94E 02	6.08E 02
3.30E 00	4.62E 02	4.73E 02
3.50E 00	3.76E 02	3.88E 02
3.71E 00	3.27E 02	3.37E 02
3.91E 00	3.01E 02	3.10E 02
4.15E 00	2.81E 02	2.89E 02
4.45E 00	2.62E 02	2.69E 02
4.75E 00	2.35E 02	2.42E 02
5.04E 00	2.04E 02	2.09E 02
5.35E 00	1.75E 02	1.80E 02
5.65E 00	1.51E 02	1.57E 02
5.94E 00	1.31E 02	1.36E 02
6.25E 00	1.08E 02	1.14E 02
6.56E 00	8.92E 01	9.46E 01
6.84E 00	7.58E 01	7.96E 01
7.24E 00	5.93E 01	6.23E 01
7.74E 00	4.12E 01	4.46E 01
8.24E 00	2.96E 01	3.26E 01
8.76E 00	2.27E 01	2.48E 01
9.26E 00	1.95E 01	2.14E 01
9.74E 00	1.60E 01	1.79E 01
1.03E 01	1.17E 01	1.33E 01
1.08E 01	8.37E 00	9.77E 00
1.12E 01	6.24E 00	7.58E 00
1.18E 01	4.92E 00	5.99E 00
1.24E 01	4.23E 00	5.11E 00
1.32E 01	3.75E 00	4.39E 00
1.40E 01	2.67E 00	3.10E 00
1.48E 01	1.44E 00	1.73E 00
1.56E 01	4.76E-01	7.21E-01
1.65E 01	1.89E-02	2.25E-01
1.75E 01	-1.30E-01	6.59E-02
1.85E 01	-1.64E-01	6.26E-02
1.95E 01	-1.31E-01	8.79E-02
2.06E 01	-1.19E-01	1.01E-01
2.16E 01	-8.89E-02	1.21E-01
2.26E 01	-1.03E-01	1.13E-01
2.35E 01	-1.09E-01	1.25E-01

E1 (MEV)	E2 (MEV)	INTEGRAL (N/(CM2*S*KW))	ERROR (N/(CM2*S*KW))
0.811	1.000	4.89E 02	3.35E 00
1.000	1.200	4.97E 02	2.66E 00
1.200	1.600	8.48E 02	4.60E 00
1.600	2.000	6.45E 02	3.87E 00
2.000	3.000	1.21E 03	7.41E 00
3.000	4.000	4.19E 02	5.44E 00
4.000	6.000	4.26E 02	6.29E 00
6.000	8.000	1.48E 02	4.20E 00
8.000	10.000	4.62E 01	2.21E 00
10.000	12.000	1.71E 01	1.36E 00
12.000	16.000	1.11E 01	9.93E-01
16.000	20.000	6.35E-02	4.26E-01
1.500	15.000	3.11E 03	3.27E 01
3.000	12.000	1.06E 03	1.95E 01

Table 8. Runs 1494A, 1493A, and 1492A. Hydrogen counters on center-line at 155.4 cm behind fuel pins *(Item I-A)*

N		ENERGY BOUNDARY (MEV)		FLUX (N/(CM2*S*MEV*KW))	ERROR (PERCENT)
1	1	0.0528	0.0621	4.11E 04	1.92
1	2	0.0621	0.0732	3.13E 04	2.32
1	3	0.0732	0.0861	2.99E 04	2.30
1	4	0.0861	0.1028	1.95E 04	2.99
1	5	0.1028	0.1195	1.88E 04	3.60
1	6	0.1195	0.1417	2.34E 04	2.31
1	7	0.1417	0.1658	1.78E 04	3.10
1	8	0.1658	0.1954	1.61E 04	3.00
1	9	0.1954	0.2306	1.36E 04	3.19
2	1	0.1667	0.1986	1.92E 04	1.07
2	2	0.1986	0.2306	1.70E 04	1.37
2	3	0.2306	0.2717	1.54E 04	1.27
2	4	0.2717	0.3219	1.48E 04	1.18
2	5	0.3219	0.3767	1.17E 04	1.51
2	6	0.3767	0.4452	7.23E 03	2.10
3	1	0.3259	0.3810	9.16E 03	0.72
3	2	0.3810	0.4452	7.93E 03	0.78
3	3	0.4452	0.5279	6.32E 03	0.82
3	4	0.5279	0.6197	6.58E 03	0.78
3	5	0.6197	0.7298	6.17E 03	0.74
3	6	0.7298	0.8584	4.21E 03	0.97
3	7	0.8584	1.0052	2.67E 03	1.45
3	8	1.0052	1.1889	2.12E 03	1.54
3	9	1.1889	1.4000	1.93E 03	1.58

Table 9. Measurements on centerline with Hornyak button and Bonner ball configurations *(Items I, II, III, IV)*

Item	Configuration	Detector location (cm)[a]	Hornyak button dose rate (erg/g.s.kW)	Bonner ball count rate ($s^{-1}.W^{-1}$) 2-in.-diam Foreground[b]	2-in.-diam Background[c]	5-in.-diam Foreground	5-in.-diam Background	10-in.-diam Foreground	10-in.-diam Background
I-A	Fuel pins	155.4	--	3.10(-1)[d]	2.56(-2)	2.20(1)	5.65(-1)	1.21(1)	1.90(-1)
II-A	Fuel pins + exit shield	39.8	3.36(-5)	2.06(-3)	--	6.06(-1)	2.22(-3)	3.92(-1)	--
III-	Fuel pins + exit shield (No B_4C in control rod sleeve)								
A	No control rod	39.8	2.17(-3)	3.20(-1)	--	2.08(1)	--	1.18(1)	--
B	60-cm control rod + handler	39.8	3.33(-4)	2.09(-2)	--	6.01(0)	--	3.22(0)	--
C	120-cm control rod + partial handler	39.8	1.16(-4)	4.02(-3)	--	1.95(0)	--	1.13(0)	--
D	120-cm control rod	39.8	2.29(-5)	1.93(-3)	--	4.00(-1)	--	4.60(-1)	--
IV-	Fuel pins + exit shield (B_4C in control rod sleeve)								
A	No control rod	39.8	1.64(-3)	2.98(-1)	--	1.69(1)	--	9.42(0)	--
B	60-cm control rod + handler	39.8	1.81(-4)	1.15(-2)	--	4.01(0)	--	2.05(0)	--
C	120-cm control rod + partial handler	39.8	3.83(-5)	1.88(-3)	--	7.04(-1)	--	4.73(-1)	--
D	120-cm control rod	39.8	1.67(-5)	1.38(-3)	--	2.28(-1)	--	2.01(-1)	

[a] Distance behind configuration
[b] Neutron flux without shadow shield between configuration
[c] Neutron flux with shadow shield between configuration
[d] Read: 3.10×10^{-1}

Table 10. Run 7821B. NE-213 on centerline at 39.8 cm behind fuel pins plus exit shield *(Item II-A)*

NEUTRON ENERGY (MEV)	FLUX (N/(CM2*S*MEV*KW)) LOWER LIMIT	UPPER LIMIT	NEUTRON ENERGY (MEV)	FLUX (N/(CM2*S*MEV*KW)) LOWER LIMIT	UPPER LIMIT
8.11E-01	8.46E 01	8.62E 01	5.94E 00	3.28E 00	3.42E 00
9.07E-01	1.17E 02	1.19E 02	6.25E 00	2.77E 00	2.95E 00
1.01E 00	1.08E 02	1.09E 02	6.56E 00	2.34E 00	2.50E 00
1.11E 00	8.56E 01	8.63E 01	6.84E 00	2.02E 00	2.12E 00
1.20E 00	6.83E 01	6.90E 01	7.24E 00	1.67E 00	1.77E 00
1.31E 00	5.68E 01	5.74E 01	7.74E 00	1.28E 00	1.39E 00
1.41E 00	5.03E 01	5.09E 01	8.24E 00	9.67E-01	1.06E 00
1.51E 00	4.64E 01	4.70E 01	8.76E 00	7.43E-01	8.11E-01
1.61E 00	4.33E 01	4.38E 01	9.26E 00	5.36E-01	5.95E-01
1.71E 00	4.06E 01	4.11E 01	9.74E 00	3.89E-01	4.47E-01
1.81E 00	3.86E 01	3.91E 01	1.03E 01	3.32E-01	3.83E-01
1.93E 00	3.74E 01	3.78E 01	1.08E 01	2.97E-01	3.43E-01
2.10E 00	3.59E 01	3.63E 01	1.12E 01	2.53E-01	2.95E-01
2.30E 00	3.17E 01	3.21E 01	1.18E 01	2.10E-01	2.47E-01
2.50E 00	2.56E 01	2.59E 01	1.24E 01	1.69E-01	2.01E-01
2.70E 00	2.03E 01	2.06E 01	1.32E 01	1.25E-01	1.47E-01
2.90E 00	1.67E 01	1.71E 01	1.40E 01	7.62E-02	9.19E-02
3.10E 00	1.37E 01	1.41E 01	1.48E 01	3.55E-02	4.60E-02
3.30E 00	1.13E 01	1.15E 01	1.56E 01	7.56E-03	1.87E-02
3.50E 00	9.51E 00	9.84E 00	1.65E 01	-2.67E-03	6.43E-03
3.71E 00	8.55E 00	8.81E 00	1.75E 01	-5.30E-03	3.43E-03
3.91E 00	8.02E 00	8.24E 00	1.85E 01	-6.15E-03	3.92E-03
4.15E 00	7.39E 00	7.61E 00	1.95E 01	-5.33E-03	4.43E-03
4.45E 00	6.48E 00	6.66E 00	2.06E 01	-5.32E-03	4.46E-03
4.75E 00	5.68E 00	5.86E 00	2.16E 01	-4.04E-03	5.33E-03
5.04E 00	4.86E 00	5.01E 00	2.26E 01	-4.60E-03	5.03E-03
5.35E 00	4.17E 00	4.31E 00	2.35E 01	-4.80E-03	5.61E-03
5.65E 00	3.71E 00	3.87E 00			

E1 (MEV)	E2 (MEV)	INTEGRAL (N/(CM2*S*KW))	ERROR (N/(CM2*S*KW))
0.811	1.000	2.09E 01	9.15E-02
1.000	1.200	1.77E 01	6.87E-02
1.200	1.600	2.12E 01	1.16E-01
1.600	2.000	1.59E 01	9.62E-02
2.000	3.000	2.62E 01	1.87E-01
3.000	4.000	1.04E 01	1.44E-01
4.000	6.000	1.05E 01	1.71E-01
6.000	8.000	4.04E 00	1.24E-01
8.000	10.000	1.39E 00	6.85E-02
10.000	12.000	5.93E-01	4.42E-02
12.000	16.000	3.71E-01	3.74E-02
16.000	20.000	4.81E-04	1.89E-02
1.500	15.000	7.38E 01	8.93E-01
3.000	12.000	2.69E 01	5.52E-01

Table 11. Runs 1496A, 1496B, and 1495B. Hydrogen counters on centerline at 155.4 cm behind fuel pins plus exit shield *(Item II-A)*

K	ENERGY BOUNDARY (MEV)		FLUX (N/(CM2*S*MEV*KW))	ERROR (PERCENT)
1	0.0452	0.0526	1.05E 03	4.99
2	0.0526	0.0618	7.14E 02	6.59
3	0.0618	0.0729	8.02E 02	5.50
4	0.0729	0.0858	9.18E 02	4.57
5	0.0858	0.1006	6.89E 02	5.88
6	0.1006	0.1190	6.90E 02	5.13
7	0.1190	0.1393	8.40E 02	4.21
8	0.1393	0.1652	6.75E 02	4.27
9	0.1397	0.1672	6.68E 02	1.68
10	0.1652	0.1947	5.53E 02	4.88
11	0.1672	0.1947	5.56E 02	2.29
12	0.1947	0.2314	4.79E 02	2.16
13	0.1987	0.2356	5.23E 02	0.61
14	0.2314	0.2726	4.21E 02	2.44
15	0.2356	0.2726	4.61E 02	0.78
16	0.2726	0.3188	3.26E 02	0.98
17	0.3188	0.3835	3.59E 02	0.71
18	0.3835	0.4482	2.92E 02	0.99
19	0.4482	0.5221	2.44E 02	1.14
20	0.5221	0.6145	2.70E 02	0.88
21	0.6145	0.7254	2.57E 02	0.81
22	0.7254	0.8548	1.93E 02	0.96
23	0.8548	1.0119	1.49E 02	1.05
24	1.0119	1.1875	9.92E 01	1.45
25	1.1875	1.4000	6.17E 01	1.96

Table 12. Radial traverses in the horizontal plane behind the fuel pins plus exit shield *(Item II-A)*

Distance from centerline (cm)	Bonner ball at 39.8-cm count rate ($s^{-1}.W^{-1}$)		Distance from centerline (cm)	0.635-cm-diam Hornyak button at 1.9-cm dose rate (erg/g.s.kW)
	2-in.-diam	5-in.-diam		
60.0 N	9.77(-4)[a]	7.72(-2)	42.0 N	5.03(-6)[a]
57.5	--	8.75(-2)	37.0	9.75(-6)
55.0	--	9.34(-2)	32.0	2.24(-5)
52.5	--	1.02(-1)	30.5	3.86(-5)
50.0	1.21(-3)	1.12(-1)	30.0	1.40(-4)
47.5	--	1.24(-1)	29.6	1.67(-4)
45.0	1.32(-3)	1.34(-1)	29.0	1.43(-4)
42.5	--	1.47(-1)	28.5	4.08(-5)
40.0	1.48(-3)	1.68(-1)	28.0	3.92(-5)
37.5	--	1.97(-1)	27.0	5.03(-5)
37.0	1.54(-3)	--	26.0	7.97(-5)
35.0	1.62(-3)	2.97(-1)	25.0	1.04(-4)
34.0	1.65(-3)	--	24.0	9.56(-5)
33.0	1.77(-3)	--	23.0	8.72(-5)
32.5	--	4.63(-1)	22.0	8.31(-5)
32.0	4.58(-3)	--	21.0	8.06(-5)
31.0	9.57(-3)	--	20.0	7.75(-5)
30.0	1.25(-2)	5.56(-1)	19.0	8.06(-5)
29.0	1.27(-2)	--	18.0	8.03(-5)
28.0	8.87(-3)	--	17.0	8.00(-5)
27.5	--	5.82(-1)	16.0	8.42(-5)
27.0	4.01(-3)	--	15.0	9.44(-5)
26.0	2.30(-3)	--	14.0	1.02(-4)
25.0	2.21(-3)	5.34(-1)	13.0	8.47(-5)
24.0	2.07(-3)	--	12.0	5.86(-5)
23.0	2.02(-3)	--	11.0	4.58(-5)
22.5	--	4.61(-1)	10.0	7.44(-5)
22.0	1.99(-3)	--	9.75	1.10(-4)
21.0	1.99(-3)	--	9.5	1.29(-4)
20.0	2.02(-3)	4.74(-1)	9.25	9.22(-5)
19.0	2.03(-3)	--	9.0	5.58(-5)
18.0	2.03(-3)	--	8.0	5.58(-5)
17.5	--	5.12(-1)	7.0	7.72(-5)
17.0	2.07(-3)	--	6.0	1.16(-4)
16.0	2.20(-3)	--	5.0	1.27(-4)
15.0	2.43(-3)	5.74(-1)	4.0	1.26(-4)
14.0	2.66(-3)	--	3.0	1.14(-4)
13.0	2.71(-3)	--	2.0	9.83(-5)
12.5	--	6.54(-1)	1.0	9.44(-5)
12.0	3.05(-3)	--	0	9.86(-5)
11.0	3.78(-3)	--	1.0 S	9.19(-5)
10.0	3.95(-3)	7.25(-1)	2.0	9.33(-5)
9.0	4.02(-3)	--	3.0	9.67(-5)
8.0	3.60(-3)	--	4.0	9.53(-5)
7.5	--	7.25(-1)	5.0	1.00(-4)
7.0	3.12(-3)	--	6.0	9.50(-5)
6.0	3.17(-3)	--	7.0	6.56(-5)
5.0	2.98(-3)	6.95(-1)	8.0	5.22(-5)
4.0	2.67(-3)	--	9.0	4.94(-5)
2.5	--	6.42(-1)	9.5	8.67(-5)
2.0	2.17(-3)	--	9.75	1.14(-4)
0	2.06(-3)	6.06(-1)	10.0	1.18(-4)
2.0 S	2.03(-3)	--	10.25	8.31(-5)
2.5	--	5.70(-1)	11.0	4.86(-5)
4.0	2.05(-3)	--	12.0	5.31(-5)

Table 12. (continued)

Distance from centerline (cm)	Bonner ball at 39.8-cm count rate ($s^{-1}.W^{-1}$)	
	2-in.-diam	5-in.-diam
5.0	--	5.92(-1)
6.0	2.08(-5)	--
7.0	2.21(-5)	--
7.5	--	6.29(-1)
8.0	3.07(-5)	--
9.0	3.56(-5)	--
10.0	3.90(-5)	6.83(-1)
11.0	3.89(-5)	--
12.0	3.44(-5)	--
12.5	--	6.80(-1)
13.0	3.40(-5)	--
14.0	3.31(-5)	--
15.0	2.94(-5)	6.21(-1)
16.0	2.52(-5)	--
17.0	2.25(-5)	--
17.5	--	5.52(-1)
18.0	2.05(-5)	--
19.0	2.05(-5)	--
20.0	--	4.90(-1)
21.0	1.97(-5)	--
22.5	--	4.36(-1)
23.0	1.96(-5)	--
25.0	1.95(-5)	4.53(-1)
26.0	1.95(-5)	--
27.0	3.11(-5)	--
27.5	--	4.92(-1)
28.0	7.17(-5)	--
29.0	9.18(-5)	--
30.0	9.35(-5)	4.77(-1)
31.0	7.24(-5	--
32.0	3.06(-5)	--
32.5	--	4.06(-1)
33.0	1.69(-5)	--
34.0	1.62(-5)	--
35.0	--	2.98(-1)
36.0	1.56(-5)	--
37.5	--	1.99(-1)
40.0	--	1.72(-1)
42.0	1.39(-5)	--
42.5	--	1.51(-1)
45.0	--	1.37(-1)
47.5	--	1.25(-1)
48.0	1.25(-5)	--
50.0	--	1.11(-1)
52.5	--	1.00(-1)
54.0	1.12(-3)	--
60.0	9.65(-4)	7.81(-2)

Distance from centerline (cm)	0.635-cm-diam Hornyak button at 1.9-cm dose rate (erg/g.s.kW)
13.0	7.78(-5)
14.0	1.19(-4)
15.0	1.22(-4)
16.0	1.07(-4)
17.0	8.86(-5)
19.0	8.42(-5)
21.0	7.44(-5)
23.0	7.89(-5)
24.0	8.06(-5)
25.0	8.03(-5)
26.0	7.42(-5)
28.0	3.67(-5)
28.5	3.33(-5)
29.0	6.33(-5)
29.5	1.22(-4)
30.0	1.26(-4)
30.5	6.92(-5)
32.0	2.09(-5)
35.0	1.28(-5)

[a] Read: 9.77×10^{-4}

Table 13. Axial traverses with Hornyak button and 2-in. Bonner ball along the centerline of the control rod sleeve *(Items III-A, IV-A)*

Distance from shadow shield (cm)	2-in.-diam Bonner ball count rate ($s^{-1}.W^{-1}$)		Distance from shadow shield (cm)	0.635-cm-diam Hornyak button dose rate (erg/g.s.kW)	
	Item III-A[a]	Item IV-A[b]		Item III-A[c]	Item IV-A[d]
5.0	--	4.97(2)[e]	1.2	--	1.19(0)
5.4	5.35(2)	--	3.5	1.54(0)	--
10.0	--	4.36(2)	6.4	--	1.25(0)
10.6	4.35(2)	--	8.5	1.53(0)	--
15.0	--	3.71(2)	11.3	--	1.18(0)
15.4	3.79(2)	--	13.5	1.48(0)	--
20.0	--	3.26(2)	16.2	--	1.12(0)
20.4	3.25(2)	--	18.5	1.31(0)	--
25.4	2.89(2)	--	21.2	--	9.97(-1)
30.0	--	2.53(2)	23.5	1.21(0)	--
35.5	2.35(2)	--	31.2	--	8.08(-1)
55.0	--	1.60(2)	33.5	9.31(-1)	--
55.4	1.71(2)	--	51.2	--	5.75(-1)
75.4	1.19(2)	--	53.5	6.75(-1)	--
80.0	--	8.04(1)	73.5	4.50(-1)	--
90.0	--	3.37(1)	76.2	--	3.69(-1)
95.4	6.57(1)	--	93.5	2.73(-1)	--
100.0	--	1.48(1)	101.2	--	1.63(-1)
115.4	2.98(1)	--	113.5	1.32(-1)	--
125.0	--	4.52(0)	126.2	--	5.53(-2)
125.4	1.81(1)	--	133.5	5.77(-2)	--
135.4	9.02(0)	--	151.2	--	1.64(-2)
145.4	4.79(0)	--	153.5	2.33(-2)	--
150.0	--	1.74(0)	173.5	1.11(-2)	--
165.4	1.98(0)	--	176.2	--	6.78(-3)
175.0	--	9.32(-1)	193.5	6.53(-3)	--
185.4	1.10(0)	--	201.2	--	3.92(-3)
200.0	--	5.91(-1)	213.5	4.14(-3)	--
205.4	6.94(-1)	--	223.5	3.36(-3)	--
215.7	5.24(-1)	--	226.2	--	2.32(-3)
225.0	--	3.83(-1)	243.5	2.42(-3)	--
225.4	4.44(-1)	--	246.2	--	1.73(-3)
235.4	3.83(-1)	--	253.5	2.12(-3)	--
245.0	--	3.06(-1)	256.2	--	1.57(-3)
245.4	3.36(-1)	--	263.5	1.84(-3)	--
255.0	--	2.71(-1)			
275.4	2.89(-1)	--			

[a]No B_4C in sleeve
[b]B_4C in sleeve
[c]No B_4C in sleeve
[d]B_4C in sleeve
[e]Read: 4.97×10^2

Table 14. Radial traverses in the horizontal plane with the Hornyak button at 1.9 cm behind fuel pins plus exit shield for several control rod positions (no B_4C in control rod sleeve) *(Items III-A, III-B, III-C, III-D)*

Distance from centerline (cm)	Dose rate (erg/g.s.kW)			
	Item III-A[a]	Item III-B[b]	Item III-C[c]	Item III-D[d]
60.0 N	3.50(-6)[e]	--	1.14(-6)	1.14(-6)
50.0	6.86(-6)	--	2.72(-6)	--
40.0	2.56(-5)	1.46(-5)	8.22(-6)	5.42(-6)
38.0	3.39(-5)	--	--	--
36.0	4.50(-5)	--	--	--
35.0	--	2.69(-5)	1.76(-5)	9.67(-6)
34.0	6.36(-5)	--	--	--
33.0	--	3.94(-5)	--	--
32.5	--	--	2.69(-5)	1.63(-5)
32.0	9.19(-5)	--	--	--
31.25	--	--	3.53(-5)	1.98(-5)
31.0	1.06(-4)	5.81(-5)	--	--
30.5	1.25(-4)	--	3.83(-5)	--
30.0	2.04(-4)	1.40(-4)	8.58(-5)	8.45(-5)
29.5	2.54(-4)	1.91(-4)	1.56(-4)	1.33(-4)
29.0	2.32(-4)	1.87(-4)	1.76(-4)	--
28.75	--	--	--	8.47(-5)
28.5	--	9.39(-5)	1.06(-4)	--
28.25	--	--	5.53(-5)	--
28.0	1.57(-4)	8.31(-5)	--	--
27.5	--	--	5.81(-5)	3.11(-5)
27.0	--	1.04(-4)	--	--
26.0	2.59(-4)	1.41(-4)	--	6.00(-5)
25.0	--	1.69(-4)	1.16(-4)	7.67(-5)
24.0	3.00(-4)	1.70(-4)	--	--
22.5	--	--	1.10(-4)	6.67(-5)
22.0	2.97(-4)	1.61(-4)	--	--
21.0	--	1.59(-4)	--	--
20.0	3.33(-4)	1.64(-4)	1.08(-4)	6.06(-5)
19.0	--	1.72(-4)	--	--
18.0	3.50(-4)	--	--	--
17.5	--	--	1.10(-4)	6.25(-5)
17.0	--	1.67(-4)	--	--
16.0	3.50(-4)	--	--	--
15.0	3.61(-4)	1.83(-4)	1.23(-4)	7.53(-5)
14.0	3.58(-4)	--	--	8.61(-5)
13.0	3.75(-4)	1.82(-4)	--	--
12.5	--	--	1.13(-4)	5.56(-5)
12.0	4.44(-4)	--	--	--
11.25	--	--	--	4.17(-5)
11.0	6.17(-4)	2.27(-4)	--	--
10.0	9.81(-4)	3 56(-4)	1.67(-4)	8.15(-5)
9.5	--	--	2.42(-4)	--
9.25	--	--	--	1.41(-4)
9.0	--	5.22(-4)	2.55(-4)	--
8.75	--	--	2.97(-4)	2.00(-4)
8.0	3.36(-3)	7.33(-4)	--	--
7.5	--	--	2.78(-4)	4.61(-5)
7.0	--	8.17(-4)	--	--
6.0	4.08(-3)	8.14(-4)	--	--
5.0	--	8.28(-4)	2.89(-4)	4.06(-5)
4.0	--	8.00(-4)	--	--
3.0	--	7.75(-4)	--	--
2.5	--	--	2.48(-4)	--

Table 14. (continued)

Distance from centerline (cm)	Dose rate (erg/g.s.kW)			
	Item III-A	Item III-B	Item III-C	Item III-D
2.0	4.25(-3)	6.56(-4)	--	--
1.25	--	--	1.30(-4)	--
1.0	--	2.89(-4)	--	--
0	4.42(-3)	2.56(-4)	1.08(-4)	4.14(-5)
0.9 S	--	2.59(-4)	--	--
1.25	--	--	1.09(-4)	--
1.9	--	4.47(-4)	--	--
2.0	4.17(-3)	--	--	--
2.5	--	--	1.23(-4)	--
2.9	--	6.78(-4)	--	--
3.75	--	--	2.06(-4)	--
4.0	4.11(-3)	7.33(-4)	--	--
5.0	--	7.78(-4)	2.60(-4)	4.31(-5)
6.0	4.08(-3)	7.81(-4)	--	--
7.0	--	7.67(-4)	--	--
7.5	--	7.44(-4)	2.67(-4)	4.61(-5)
8.0	3.65(-3)	--	--	--
8.75	--	--	--	1.33(-5)
9.0	--	5.47(-4)	--	1.79(-5)
9.5	--	--	--	1.23(-5)
10.0	1.18(-3)	4.14(-4)	2.39(-4)	1.27(-4)
11.0	--	2.58(-4)	--	--
11.25	--	--	--	4.47(-5)
11.5	--	--	1.12(-4)	--
12.0	4.56(-4)	1.81(-4)	1.00(-4)	--
12.5	--	--	1.04(-4)	5.08(-5)
13.0	3.94(-4)	1.81(-4)	--	--
13.75	--	--	1.33(-4)	8.72(-5)
14.0	3.75(-4)	2.03(-4)	--	--
15.0	3.81(-4)	--	1.44(-4)	1.01(-4)
16.0	3.78(-4)	2.00(-4)	--	--
16.25	--	--	--	9.22(-5)
16.75	--	--	1.31(-4)	--
17.0	3.64(-4)	--	--	--
17.5	--	--	--	7.31(-5)
18.0	3.56(-4)	1.75(-4)	--	--
20.0	3.47(-4)	1.65(-4)	1.07(-4)	6.19(-5)
22.0	3.00(-4)	1.51(-4)	--	--
22.5	--	--	1.01(-4)	6.08(-5)
24.0	2.86(-4)	1.54(-4)	--	--
25.0	--	1.56(-4)	1.06(-4)	6.83(-5)
26.0	2.68(-4)	1.40(-4)	--	--
26.25	--	--	--	6.08(-5)
27.0	--	1.11(-4)	--	--
27.5	--	--	7.00(-5)	3.58(-5)
28.0	1.69(-4)	8.69(-5)	--	--
28.75	--	--	--	2.74(-5)
29.0	1.79(-4)	9.06(-5)	5.08(-5)	--
29.25	--	--	--	6.67(-5)
29.5	2.23(-4)	1.49(-4)	9.89(-5)	--
29.75	2.25(-4)	--	--	--
30.0	--	1.56(-4)	1.36(-4)	1.05(-4)
30.3	1.83(-4)	--	--	--
30.5	1.24(-4)	8.81(-5)	1.14(-4)	5.25(-5)
31.0	1.14(-4)	--	--	--
31.25	--	--	--	1.97(-5)

Table 14. (continued)

Distance from centerline (cm)	Dose rate (erg/g.s.kW)			
	Item III-A	Item III-B	Item III-C	Item III-D
32.0	--	4.94(-5)	--	--
32.5	--	--	2.94(-5)	1.59(-5)
33.0	7.72(-5)	--	--	--
34.0	--	3.28(-5)	--	--
35.0	5.72(-5)	--	1.93(-5)	1.01(-5)
36.0	--	2.56(-5)	--	--
40.0	2.86(-5)	1.42(-5)	9.81(-6)	5.03(-6)
50.0	8.08(-6)	--	--	--
60.0	2.83(-6)	--	--	--

[a]No control rod
[b]60-cm control rod and handler
[c]120-cm control rod and handler
[d]120-cm control rod
[e]Read: 3.50×10^{-6}

Table 15. Radial traverses in the horizontal plane with the 2-in. Bonner ball at 39.8 cm behind the fuel pins plus exit shield for several **control** rod positions (no B_4C in control rod sleeve) *(Items III-A, III-B, III-C, III-D)*

Distance from centerline (cm)	Count rate ($s^{-1}.W^{-1}$)			
	Item III-A[a]	Item III-B[b]	Item III-C[c]	Item III-D[d]
60.0 N	3.82(-3)[e]	1.92(-3)	1.22(-3)	9.32(-4)
50.0	4.91(-3)	2.46(-3)	1.51(-3)	1.14(-3)
45.0	5.60(-3)	2.67(-3)	1.67(-3)	--
40.0	6.27(-3)	3.00(-3)	1.85(-3)	1.36(-3)
35.0	7.09(-3)	3.30(-3)	2.06(-3)	1.49(-3)
33.5	--	3.49(-3)	--	--
33.25	--	--	2.16(-3)	--
32.5	7.93(-3)	5.87(-3)	3.25(-3)	2.72(-3)
31.25	1.22(-2)	1.19(-2)	8.38(-3)	8.45(-3)
30.0	1.70(-2)	1.26(-2)	1.17(-2)	1.09(-2)
29.5	1.75(-2)	--	--	--
29.0	1.77(-2)	--	--	--
28.75	--	1.11(-2)	--	--
28.5	1.74(-2)	--	9.23(-3)	--
28.25	--	--	--	9.12(-3)
27.5	1.42(-2)	5.33(-3)	5.54(-3)	4.94(-3)
26.5	--	4.21(-3)	--	--
26.25	--	--	3.23(-3)	--
25.0	9.25(-3)	4.04(-3)	2.64(-3)	2.04(-3)
22.5	9.66(-3)	4.01(-3)	2.45(-3)	1.83(-3)
20.0	1.07(-2)	4.42(-3)	2.59(-3)	1.90(-3)
17.5	1.32(-2)	4.95(-3)	--	1.94(-3)
15.0	1.91(-2)	6.88(-3)	3.29(-3)	2.30(-3)
12.5	4.22(-2)	1.30(-2)	4.15(-3)	2.96(-3)
11.25	--	2.16(-2)	7.04(-3)	6.58(-3)
10.0	1.60(-1)	2.61(-2)	1.12(-2)	1.04(-2)
8.75	--	3.03(-2)	--	--
8.25	2.39(-1)	--	1.08(-2)	1.02(-2)
7.5	2.98(-1)	2.74(-2)	8.18(-3)	6.79(-3)
6.25	--	--	4.62(-3)	2.21(-3)
5.0	3.20(-1)	2.43(-2)	4.18(-3)	1.91(-3)
2.5	3.19(-1)	2.21(-2)	--	--
0	3.20(-1)	2.06(-2)	4.02(-3)	1.93(-3)
2.5 S	3.19(-1)	2.27(-2)	--	--
5.0	3.18(-1)	2.39(-2)	4.01(-3)	1.96(-3)
6.25	--	--	4.47(-3)	2.76(-3)
7.5	3.03(-1)	2.71(-2)	7.94(-3)	6.68(-3)
8.25	--	--	--	8.07(-3)
8.75	2.56(-1)	2.51(-2)	9.38(-3)	--
10.0	1.78(-1)	2.18(-2)	8.55(-3)	8.32(-3)
11.25	--	--	6.04(-3)	4.99(-3)
12.5	5.27(-2)	9.56(-2)	4.45(-3)	3.40(-3)
15.0	2.12(-2)	6.38(-3)	3.76(-3)	2.95(-3)
17.5	1.36(-2)	4.79(-3)	2.83(-3)	2.06(-3)
20.0	1.12(-2)	4.33(-3)	2.56(-3)	1.87(-3)
22.5	9.85(-3)	3.98(-3)	--	1.81(-3)
25.0	9.05(-3)	3.88(-3)	2.41(-3)	1.83(-3)
26.25	--	4.11(-3)	2.43(-3)	--
27.0	9.06(-3)	--	--	--
27.5	--	7.88(-3)	5.32(-3)	4.56(-3)
28.0	1.16(-2)	--	--	--
28.25	--	--	--	6.97(-3)
28.75	--	9.50(-3)	8.29(-3)	--
29.0	1.40(-2)	--	--	--
30.0	1.41(-2)	9.52(-3)	7.99(-3)	7.91(-3)

Table 15. (continued)

Distance from centerline (cm)	Count rate ($s^{-1}.W^{-1}$)			
	Item III-A	Item III-B	Item III-C	Item III-D
31.0	1.29(-2)	6.73(-3)	--	--
31.25	--	--	5.45(-3)	4.08(-3)
32.5	8.59(-3)	3.49(-3)	2.22(-3)	1.71(-3)
35.0	7.24(-3)	3.22(-3)	2.00(-3)	1.47(-3)
40.0	6.39(-3)	2.93(-3)	1.82(-3)	1.33(-3)
45.0	5.63(-3)	2.73(-3)	1.67(-3)	--
50.0	4.96(-3)	2.40(-3	1.51(-3)	1.14(-3)
55.0	4.38(-3)	--	--	--
60.0	4.00(-3)	1.88(-3)	1.21(-3)	9.23(-4)

[a]No control rod
[b]60-cm control rod and handler
[c]120-cm control rod and handler
[d]120-cm control rod
[e]Read: 3.82 X 10^{-3}

Table 16. Radial traverses in the horizontal plane with the 5-in. Bonner ball at 39.8 cm behind the fuel pins plus exit shield for several control rod positions (no B_4C in control rod sleeve) *(Items III-A, III-B, III-C, III-D)*

Distance from centerline (cm)	Count rate (s^{-1}, W^{-1})			
	Item III-A[a]	Item III-B[b]	Item III-C[c]	Item III-D[d]
60.0 N	4.42(-1)[e]	2.18(-1)	1.24(-1)	7.40(-2)
55.0	5.32(-1)	--	--	--
50.0	6.53(-1)	3.28(-1)	1.82(-1)	1.06(-1)
45.0	8.07(-1)	--	2.29(-1)	--
40.0	1.00(0)	5.05(-1)	2.82(-1)	1.66(-1)
35.0	1.33(0)	7.22(-1)	4.39(-1)	3.14(-1)
32.5	1.56(0)	8.96(-1)	5.73(-1)	4.41(-1)
31.25	--	--	--	4.93(-1)
30.0	1.77(0)	1.00(0)	6.48(-1)	5.30(-1)
27.5	1.90(0)	1.07(0)	6.91(-1)	5.20(-1)
25.0	2.03(0)	1.08(0)	6.68(-1)	4.69(-1)
22.5	2.35(0)	1.18(0)	6.57(-1)	--
20.0	3.05(0)	1.48(0)	7.78(-1)	4.50(-1)
17.5	4.31(0)	--	--	4.98(-1)
15.0	6.75(0)	2.83(0)	1.21(0)	6.57(-1)
12.5	--	3.95(0)	1.54(0)	8.44(-1)
11.25	--	--	--	9.18(-1)
10.0	1.43(1)	5.06(0)	1.85(0)	9.36(-1)
8.25	--	--	--	8.91(-1)
7.5	1.75(1)	5.75(0)	2.01(0)	8.29(-1)
5.0	2.01(1)	6.00(0)	2.02(0)	6.28(-1)
2.5	--	6.00(0)	1.94(0)	4.10(-1)
0	2.08(1)	6.01(0)	1.95(0)	4.00(-1)
2.5 S	--	5.98(0)	1.88(0)	4.57(-1)
5.0	1.95(1)	5.74(0)	1.99(0)	6.98(-1)
7.5	1.66(1)	5.34(0)	1.95(0)	8.74(-1)
8.5	--	--	--	9.26(-1)
10.0	1.33(1)	4.38(0)	1.77(0)	9.46(-1)
11.0	--	--	--	9.14(-1)
12.5	--	--	1.53(0)	8.34(-1)
15.0	5.93(0)	2.37(0)	1.17(0)	6.37(-1)
17.5	--	--	--	5.09(-1)
20.0	2.77(0)	1.34(0)	7.57(-1)	4.42(-1)
21.25	--	--	--	4.15(-1)
22.5	2.18(0)	1.08(0)	6.34(-1)	3.95(-1)
25.0	1.93(0)	1.01(0)	6.21(-1)	4.28(-1)
27.5	1.77(0)	9.70(-1)	6.20(-1)	4.42(-1)
28.75	--	--	--	4.43(-1)
30.0	1.63(0)	8.97(-1)	5.69(-1)	4.28(-1)
32.5	1.46(0)	7.84(-1)	4.97(-1)	--
35.0	1.24(0)	6.41(-1)	3.87(-1)	2.55(-1)
40.0	9.84(-1)	4.90(-1)	2.76(-1)	1.53(-1)
45.0	7.79(-1)	--	2.19(-1)	--
50.0	6.36(-1)	3.24(-1)	1.79(-1)	1.07(-1)
55.0	5.25(-1)	--	--	--
60.0	4.34(-1)	--	1.20(-1)	7.29(-2)
80.0	--	--	--	3.81(-2)

[a] No control rod
[b] 60-cm control rod and handler
[c] 120-cm control rod and handler
[d] 120-cm control rod
[e] Read: 4.42×10^{-1}

Table 17. Radial traverses in the horizontal plane with the Hornyak button at 39.8 cm behind the fuel pins plus exit shield for several control rod positions (B_4C in control rod sleeve) *(Items IV-A, IV-B, IV-C, IV-D)*

Distance from centerline (cm)	Dose rate (erg/g.s.kW)			
	Item IV-A[a]	Item IV-B[b]	Item IV-C[c]	Item IV-D[d]
60.0 N	2.02(-6)[e]	1.30(-6)	9.92(-7)	--
50.0	5.36(-6)	--	--	--
40.0	1.37(-5)	7.31(-6)	5.53(-6)	4.78(-6)
35.0	2.94(-5)	1.64(-5)	1.17(-5)	8.58(-6)
32.5	4.36(-5)	2.28(-5)	1.79(-5)	1.42(-5)
31.5	--	--	2.13(-5)	--
31.25	--	3.06(-5)	--	1.82(-5)
31.0	5.36(-5)	--	2.27(-5)	--
30.5	--	--	3.08(-5)	3.14(-5)
30.0	1.35(-4)	1.16(-4)	9.97(-5)	1.16(-4)
29.5	1.74(-4)	1.49(-4)	1.33(-4)	1.34(-4)
29.0	1.61(-4)	1.20(-4)	1.12(-4)	1.13(-4)
28.5	--	--	3.08(-5)	--
28.0	8.28(-5)	4.61(-5)	3.11(-5)	--
27.5	--	--	--	2.92(-5)
27.0	1.04(-4)	5.53(-5)	3.83(-5)	--
26.0	--	8.14(-5)	6.03(-5)	5.69(-5)
25.0	1.64(-4)	9.81(-5)	7.61(-5)	7.39(-5)
24.0	--	9.92(-5)	7.53(-5)	--
23.0	--	9.81(-5)	--	--
22.5	1.53(-4)	--	--	5.86(-5)
22.0	--	--	6.08(-5)	--
21.0	--	8.69(-5)	--	--
20.0	1.62(-4)	--	6.19(-5)	5.22(-5)
19.0	--	8.81(-5)	--	--
17.5	1.76(-4)	--	6.22(-5)	5.25(-5)
17.0	--	8.83(-5)	--	--
16.5	1.73(-4)	--	--	--
16.0	1.82(-4)	--	--	--
15.5	1.75(-4)	--	--	--
15.0	1.87(-4)	1.03(-4)	7.50(-5)	6.97(-5)
14.5	1.97(-4)	--	--	--
14.0	--	1.11(-4)	--	7.75(-5)
13.75	--	--	8.28(-5)	--
13.5	1.93(-4)	--	--	--
13.0	--	9.39(-5)	--	--
12.5	1.95(-4)	--	5.75(-5)	4.67(-5)
12.0	1.96(-4)	7.89(-5)	--	--
11.5	--	--	4.58(-5)	--
11.25	--	--	--	2.94(-5)
11.0	2.70(-4)	9.19(-5)	4.69(-5)	--
10.5	--	--	5.25(-5)	2.89(-5)
10.0	4.31(-4)	1.52(-4)	1.01(-4)	7.53(-5)
9.75	--	--	1.59(-4)	1.09(-4)
9.5	--	2.04(-4)	1.39(-4)	1.21(-4)
9.0	--	1.55(-4)	7.28(-5)	3.50(-5)
8.75	6.89(-4)	--	--	--
8.5	--	2.13(-4)	8.00(-5)	--
8.0	2.16(-3)	3.97(-4)	1.12(-4)	2.92(-5)
7.5	2.94(-3)	--	--	--
7.0	3.03(-3)	4.44(-4)	1.19(-4)	--
6.0	--	4.44(-4)	1.19(-4)	--
5.0	3.14(-3)	4.39(-4)	1.20(-4)	2.92(-5)
4.0	--	4.17(-4)	1.11(-4)	--
3.0	--	3.83(-4)	9.92(-5)	--
2.0	--	3.17(-4)	5.97(-5)	--
1.25	--	--	5.25(-5)	--
1.0	--	1.34(-4)	--	--

Table 17. (continued)

Distance from centerline (cm)	Dose rate (erg/g.s.kW)			
	Item IV-A	Item IV-B	Item IV-C	Item IV-D
0	3.14(-3)	1.28(-4)	4.92(-5)	3.11(-5)
1.0 S	--	1.29(-4)	--	--
1.25	--	--	4.64(-5)	--
2.0	--	1.32(-4)	--	--
2.5	--	--	5.47(-5)	--
3.0	--	3.97(-4)	--	--
3.75	--	--	9.28(-5)	--
4.0	--	4.36(-4)	--	--
5.0	3.08(-3)	4.56(-4)	1.06(-4)	2.86(-5)
6.0	--	4.61(-4)	1.11(-4)	--
7.0	3.06(-3)	4.64(-4)	1.12(-4)	--
7.5	3.03(-3)	--	--	2.64(-5)
8.0	2.89(-3)	4.33(-4)	1.10(-4)	--
9.0	7.03(-4)	1.75(-4)	6.81(-5)	2.72(-5)
9.5	--	1.56(-4)	8.42(-5)	6.03(-5)
9.75	--	--	--	9.89(-5)
10.0	--	1.84(-4)	1.21(-4)	1.04(-4)
10.5	--	1.18(-4)	7.00(-5)	4.86(-5)
11.0	3.11(-3)	9.72(-5)	4.86(-5)	2.83(-5)
11.5	--	--	4.67(-5)	--
11.75	--	--	--	3.19(-5)
12.0	2.21(-3)	8.19(-5)	4.69(-5)	--
12.5	--	--	5.47(-5)	4.42(-5)
13.0	1.98(-3)	9.36(-5)	--	--
13.5	--	--	7.75(-5)	--
14.0	--	1.26(-4)	--	9.86(-5)
14.5	--	1.25(-4)	9.89(-5)	--
15.0	2.15(-3)	1.19(-4)	--	9.36(-5)
15.5	--	--	9.33(-5)	--
16.0	--	1.18(-4)	--	--
17.5	1.84(-3)	--	6.78(-5)	6.42(-5)
18.0	--	9.44(-5)	--	--
20.0	1.77(-3)	8.97(-5)	6.14(-5)	5.55(-5)
22.0	--	8.47(-5)	--	--
22.5	1.61(-3)	--	6.08(-5)	5.50(-5)
23.0	--	8.75(-5)	--	--
24.0	--	8.97(-5)	--	--
25.0	1.57(-3)	9.08(-5)	6.72(-5)	6.19(-5)
26.0	--	8.33(-5)	--	5.53(-5)
26.25	1.36(-3)	--	--	--
26.5	--	--	5.72(-5)	--
27.0	--	6.11(-5)	--	--
27.5	1.03(-4)	--	3.86(-5)	3.06(-5)
28.0	9.03(-5)	4.47(-5)	--	--
28.5	8.61(-5)	--	--	2.43(-5)
28.75	--	--	2.92(-5)	--
29.0	9.53(-5)	5.33(-5)	--	3.56(-5)
29.5	1.44(-4)	1.12(-4)	9.33(-5)	1.00(-4)
30.0	1.42(-4)	1.15(-4)	1.08(-4)	1.02(-4)
30.5	7.42(-5)	4.30(-5)	2.86(-5)	3.47(-5)
31.0	5.64(-5)	3.00(-5)	2.12(-5)	--
32.5	4.69(-5)	2.31(-5)	1.57(-5)	1.27(-5)
35.0	3.06(-5)	1.57(-5)	1.02(-5)	9.22(-6)
40.0	1.67(-5)	7.17(-6)	5.17(-6)	4.33(-6)

[a] No control rod
[b] 60-cm control rod and handler
[c] 120-cm control rod and handler
[d] 120-cm control rod
[e] Read: 2.02×10^{-6}

Table 18. Radial traverses in the horizontal plane with the 2-in. Bonner ball at 39.8 cm behind the fuel pins plus exit shield for several control rod positions (B_4C in control rod sleeve) *(Items IV-A, IV-B, IV-C. IV-D)*

Distance from centerline (cm)	Count rate ($s^{-1}.W^{-1}$)			
	Item IV-A[a]	Item IV-B[b]	Item IV-C[c]	Item IV-D[d]
60.0 N	2.48(-3)[e]	1.26(-3)	9.09(-4)	7.29(-4)
50.0	2.81(-3)	--	1.09(-3)	--
40.0	3.55(-3)	1.81(-3)	1.31(-3)	1.08(-3)
35.0	4.05(-3)	2.04(-3)	1.45(-3)	1.19(-3)
32.5	6.04(-3)	3.42(-3)	3.50(-3)	1.40(-3)
31.25	1.19(-2)	9.52(-3)	9.82(-3)	4.44(-3)
30.5	--	--	--	8.27(-3)
30.0	1.45(-2)	1.18(-2)	1.06(-2)	9.81(-3)
29.5	--	--	--	1.09(-2)
29.0	--	--	--	1.13(-2)
28.75	1.30(-2)	1.04(-2)	9.70(-3)	--
28.5	--	--	--	1.08(-2)
28.0	--	--	--	9.62(-3)
27.5	7.13(-3)	5.49(-3)	3.57(-3)	--
27.0	--	--	--	5.46(-3)
25.0	5.29(-3)	2.63(-3)	1.87(-3)	1.72(-3)
23.75	--	--	1.78(-3)	--
22.5	5.51(-3)	2.44(-3)	1.72(-3)	1.51(-3)
20.0	6.03(-3)	2.53(-3)	1.78(-3)	1.51(-3)
17.5	6.60(-3)	2.66(-3)	1.80(-3)	1.52(-3)
15.0	9.41(-3)	3.24(-3)	2.27(-3)	1.70(-3)
13.75	--	--	2.43(-3)	--
12.5	3.57(-2)	5.44(-3)	2.97(-3)	2.11(-3)
11.5	--	--	--	2.61(-3)
11.25	--	9.13(-3)	4.14(-3)	--
11.0	--	--	--	3.16(-3)
10.5	--	--	--	3.52(-3)
10.0	1.69(-1)	1.21(-2)	3.93(-3)	3.67(-3)
9.5	--	--	--	3.75(-3)
9.0	--	--	3.93(-3)	3.78(-3)
8.75	--	1.49(-2)	3.67(-3)	--
8.7	2.48(-1)	--	--	--
8.5	--	--	--	3.56(-3)
8.0	--	--	--	3.16(-3)
7.5	2.85(-1)	1.49(-2)	2.26(-3)	--
7.0	--	--	--	1.99(-3)
6.25	--	1.50(-2)	--	--
5.0	2.93(-1)	1.44(-2)	2.06(-3)	1.37(-3)
2.5	--	1.31(-2)	1.96(-3)	--
0	2.98(-1)	1.12(-2)	1.88(-3)	1.38(-3)
2.5 S	--	1.37(-2)	1.97(-3)	--
5.0	2.95(-1)	1.53(-2)	2.03(-3)	1.37(-3)
6.25	--	1.56(-2)	--	--
7.0	--	--	--	1.39(-3)
7.5	2.61(-1)	1.49(-2)	3.01(-3)	--
8.0	--	--	--	1.89(-3)
8.5	--	--	--	2.53(-3)
8.75	1.96(-1)	1.39(-2)	3.69(-3)	--
9.0	--	--	--	2.97(-3)
9.5	--	--	--	3.22(-3)
10.0	1.17(-1)	1.08(-2)	3.92(-3)	3.47(-3)
10.5	--	--	--	3.62(-3)
11.0	--	--	--	3.63(-3)
11.25	--	7.87(-3)	3.55(-3)	--
11.5	--	--	--	3.54(-3)

Table 18. (continued)

Distance from centerline (cm)	Count rate ($s^{-1} \cdot W^{-1}$)			
	Item IV-A	Item IV-B	Item IV-C	Item IV-D
12.0	--	--	--	3.37(-3)
12.5	1.96(-2)	5.21(-3)	3.05(-3)	--
13.0	--	--	--	2.76(-3)
14.0	--	--	--	2.83(-3)
15.0	8.66(-3)	3.68(-3)	2.61(-3)	2.70(-3)
17.5	6.37(-3)	2.80(-3)	1.89(-3)	1.77(-3)
20.0	5.75(-3)	2.56(-3)	1.76(-3)	1.53(-3)
22.5	5.33(-3)	2.44(-3)	1.70(-3)	1.44(-3)
25.0	5.16(-3)	2.48(-3)	1.71(-3)	1.45(-3)
26.5	--	2.64(-3)	--	--
27.5	8.46(-3)	5.20(-3)	6.02(-3)	2.43(-3)
28.0	--	6.95(-3)	--	3.85(-3)
28.5	--	--	--	5.49(-3)
28.75	1.01(-2)	8.28(-3)	7.08(-3)	--
29.0	--	--	--	6.49(-3)
29.5	1.06(-2)	--	--	7.10(-3)
30.0	1.00(-2)	7.82(-3)	7.24(-3)	7.45(-3)
30.5	--	--	--	7.26(-3)
31.0	--	--	--	6.47(-3)
31.25	6.68(-3)	5.65(-3)	3.63(-3)	--
32.5	4.41(-3)	2.29(-3)	1.50(-3)	2.44(-3)
35.0	3.96(-3)	2.04(-3)	1.40(-3)	1.24(-3)
40.0	3.58(-3)	1.85(-3)	1.30(-3)	1.10(-3)
50.0	2.94(-3)	--	1.07(-3)	9.18(-4)
60.0	2.22(-3)	1.27(-3)	--	--

[a] No control rod
[b] 60-cm control rod and handler
[c] 120-cm control rod and handler
[d] 120-cm control rod
[e] Read: 1.96×10^{-2}

Table 19. Radial traverses in the horizontal plane with the 5-in. Bonner ball at 39.8 behind the fuel pins plus exit shield for several control rod positions (B_4C in control rod sleeve) *(Items IV-A, IV-B, IV-C, IV-D)*

Distance from centerline (cm)	Count rate ($s^{-1}.W^{-1}$)			
	Item IV-A[a]	Item IV-B[b]	Item IV-C[c]	Item IV-D[d]
60.0 N	2.47(-1)[e]	1.54(-1)	7.54(-2)	5.34(-2)
50.0	3.40(-1)	--	--	--
40.0	5.39(-1)	2.65(-1)	1.64(-1)	1.15(-1)
35.0	7.85(-1)	4.22(-1)	2.95(-1)	2.40(-1)
32.5	--	5.58(-1)	4.23(-1)	3.68(-1)
30.0	1.05(0)	6.56(-1)	4.92(-1)	4.45(-1)
27.5	--	6.66(-1)	4.96(-1)	4.38(-1)
25.0	1.11(0)	6.21(-1)	4.47(-1)	3.82(-1)
22.5	--	6.12(-1)	3.97(-1)	3.24(-1)
20.0	1.41(0)	6.87(-1)	4.32(-1)	3.33(-1)
17.5	--	8.52(-1)	4.89(-1)	3.61(-1)
15.0	3.71(0)	1.26(0)	5.94(-1)	4.02(-1)
12.5	6.82(0)	2.00(0)	7.23(-1)	4.30(-1)
10.0	1.07(1)	2.83(0)	8.01(-1)	4.15(-1)
7.5	1.41(1)	3.45(0)	8.51(-1)	3.57(-1)
5.0	1.65(1)	3.82(0)	7.81(-1)	2.76(-1)
2.5	1.68(1)	3.97(0)	7.15(-1)	2.28(-1)
0	1.69(1)	4.01(0)	7.04(-1)	2.28(-1)
2.5 S	1.68(1)	3.87(0)	7.13(-1)	2.35(-1)
5.0	1.55(1)	3.82(0)	7.66(-1)	2.89(-1)
7.5	1.26(1)	3.31(0)	8.11(-1)	3.90(-1)
10.0	8.91(0)	2.64(0)	7.97(-1)	4.62(-1)
12.5	5.21(0)	1.81(0)	7.13(-1)	4.76(-1)
15.0	2.74(0)	1.13(0)	5.98(-1)	4.40(-1)
17.5	--	8.05(-1)	5.01(-1)	3.92(-1)
20.0	1.29(0)	6.57(-1)	4.30(-1)	3.43(-1)
22.5	--	5.95(-1)	3.82(-1)	3.13(-1)
25.0	1.03(0)	5.77(-1)	4.04(-1)	3.38(-1)
27.5	--	5.86(-1)	4.22(-1)	3.60(-1)
30.0	8.94(-1)	5.38(-1)	4.03(-1)	3.46(-1)
32.5	--	4.62(-1)	3.35(-1)	2.85(-1)
35.0	6.70(-1)	3.52(-1)	2.40(-1)	1.92(-1)
40.0	4.80(-1)	2.58(-1)	1.58(-1)	1.11(-1)
50.0	3.51(-1)	1.72(-1)	1.05(-1)	7.40(-2)
60.0	--	1.19(-1)	--	5.20(-2)

[a] No control rod
[b] 60-cm control rod and handler
[c] 120-cm control rod and handler
[d] 120-cm control rod
[e] Read: 2.47×10^{-1}

APPENDIX B

PROGRAM PLAN

GCFR EXIT SHIELD EXPERIMENT
(Program Plan)

I. Fuel-pin Assembly (637 pins, 0.635-cm void between subassemblies)

A. Fuel-pin concrete form with seven subassemblies of 91 fuel pins each - 0.635-cm void between subassemblies.

1. Horizontal traverse perpendicular to beam centerline (approximately 60-cm each side) at 30.5 cm behind fuel pins

   a. 2- and 5-in. Bonner balls.

   b. Hornyak button (0.635 cm).

2. NE213 on centerline at 156.7 cm behind fuel-pins

3. Hydrogen counters (ID) at NE213 location.

4. 2-, 5-, and 10-in. Bonner balls at NE213 location.

II. Fuel-pin Assembly (with fuel pins) Plus Exit-shield Assembly

A. Fuel-pin concrete form with seven subassemblies of 91 pins each plus exit-shield concrete form with seven B_4C subassemblies.

1. Horizontal traverse perpendicular to beam centerline (approximately 60 cm each side) directly behind the exit shields

   a. Hornyak button (0.635 cm) as close as feasible (1.9 cm)

   b. 2- and 5-in. Bonner balls at NE213 distance (39.8 cm)

2. NE213 on centerline as close as feasible behind exit shield (39.8 cm)

3. Hydrogen counters (ID) at NE213 location.

4. Hornyak button and 10-in. Bonner ball on centerline at NE213 location.

III. Fuel-pin Assembly (with fuel pins) plus Exit-shield Assembly with Unshielded (no B_4C) Control Rod Subassembly

A. Fuel-pin concrete form with six subassemblies of 91 pins each (center subassembly replaced by empty control rod sleeve subassembly) plus exit-shield concrete form with six B_4C subassembly (center subassembly replaced by empty control rod sleeve subassembly).

1. Axial traverse from concrete shadow shield to 30.5 cm beyond exit shield
    a. 2-in. Bonner ball.
    b. Hornyak button (0.635 cm).
2. Horizontal traverses perpendicular to beam centerline (60 cm each side) behind exit-shield subassemblies
    a. Hornyak button (0.635 cm) as close as feasible (1.9 cm).
    b. 2- and 5-in. Bonner balls at 39.8 cm.
3. Centerline measurements behind exit shield
    a. Hornyak button and 10-in. Bonner balls at 39.8 cm.

B. Fuel-pin concrete form with six subassemblies (center subassembly replaced by empty control rod subassembly) plus exit-shield concrete form with six B_4C subassemblies (center subassemblies replaced by empty control rod subassembly) with 60-cm control rod plus rod follower in center subassembly. Control rod 7 cm from concrete shadow shield (rod follower fully inside exit shield).

1. Horizontal traverses perpendicular to beam centerline (60 cm each side) behind exit-shield subassemblies
    a. Hornyak button (0.635 cm) as close as feasible (1.9 cm).
    b. 2- and 5-in. Bonner balls at 39.8 cm.
2. Centerline measurements behind exit shield
    a. Hornyak button and 10-in. Bonner balls at 39.8 cm.

C. Fuel-pin concrete form with six subassemblies (center subassembly replaced by empty control rod subassembly) plus exit-shield concrete form with six B_4C subassemblies (center subassembly replaced by empty control rod subassembly) with 120-cm control rod plus partial rod follower in center subassembly. Control rod 7 cm from concrete shadow shield.

1. Horizontal traverses perpendicular to beam centerline (60 cm each side) behind exit-shield subassemblies
    a. Hornyak button (0.635 cm)as close as feasible (1.9 cm).
    b. 2-in and 5-in. Bonner balls at 39.8 cm.
2. Centerline measurements behind exit shield
    a. Hornyak button and 10-in. Bonner balls at 39.8 cm.

D. Fuel-pin concrete form with six subassemblies (center subassembly replaced by empty control rod subassembly) plus exit-shield concrete form with six B_4C subassemblies (center subassembly replaced by empty control rod subassembly) with 120-cm rod in center subassembly. Control rod 82 cm from concrete shadow shield (rod follower removed).

1. Horizontal traverses perpendicular to beam centerline (60 cm each side) behind exit-shield subassemblies

a. Hornyak button (0.635 cm) as close as feasible (1.9 cm).

b. 2- and 5-in. Bonner balls at 39.8 cm.

2. Centerline measurements behind exit shield

a. Hornyak button and 10-in. Bonner balls at 39.8 cm.

IV. Fuel-pin Assembly (with fuel pins) plus Exit-shield Assembly with Shielded (B_4C) Control Rod Subassembly

A. Fuel-pin concrete form with six subassemblies of 91 pins each (center subassembly replaced by empty control rod subassembly) plus exit-shield concrete form with six B_4C subassemblies (center subassembly replaced by boron-filled control rod sleeve subassembly).

1. Axial traverse from concrete shadow shield to 30.5 cm beyond exit shield

a. 2-in. Bonner ball

b. Hornyak button (0.635 cm).

2. Horizontal traverse perpendicular to beam centerline (60 cm each side) directly behind exit-shield subassemblies

a. Hornyak button (0.635 cm) as close as feasible (1.9 cm).

b. 2- and 5-in. Bonner balls at 39.8 cm.

3. Centerline measurements behind exit shield

a. Hornyak button and 10-in. Bonner balls at 39.8 cm.

B. Fuel-pin concrete form with six subassemblies (center subassembly replaced by empty control rod subassembly) plus exit-shield concrete form with six B_4C subassemblies (center subassembly replaced by boron-filled control rod sleeve subassembly) with 60-cm control rod follower in center subassembly. Control rod 7 cm from concrete shadow shield (rod follower fully inside exit shield).

1. Horizontal traverses perpendicular to beam centerline (60 cm each side) behind exit-shield subassemblies
   a. Hornyak button (0.635 cm) as close as feasible (1.9 cm).
   b. 2- and 5-in. Bonner balls at 39.8 cm.
2. Centerline measurements behind exit shield
   a. Hornyak button and 10-in. Bonner balls at 39.8 cm.

C. Fuel-pin concrete form with six subassemblies (center subassembly replaced by empty control rod subassembly) plus exit-shield concrete form with six B_4C subassemblies (center subassembly replaced by boron-filled control rod sleeve subassembly) with 120-cm control rod plus partial rod follower in center subassembly. Control rod 7 cm from concrete shadow shield.

1. Horizontal traverse perpendicular to beam centerline (60 cm each side) behind exit-shield subassemblies
   a. Hornyak button (0.635 cm) as close as feasible (1.9 cm).
   b. 2- and 5- in. Bonner balls at 39.8 cm.
2. Centerline measurements behind exit shield
   a. Hornyak button and 10-in. Bonner balls at 39.8 cm.

D. Fuel-pin concrete form with six subassemblies (center subassembly replaced by empty control rod subassembly) plus exit-shield concrete form with six B_4C subassemblies (center subassembly replaced by boron-filled control rod sleeve subassembly) with 120-cm control rod in center subassembly. Control rod 82 cm from concrete shadow shield.

1. Horizontal traverses perpendicular to beam centerline (60 cm each side) behind exit-shield subassemblies
   a. Hornyak button (0.635 cm) as close as feasible (1.9 cm).
   B. 2- and 5- in. Bonner balls at 39.8 cm.
2. Centerline measurements behind exit shield
   a. Hornyak button and 10-in. Bonner balls at 39.8 cm.

REFERENCES

1. General Atomic Company Project Staff, *300-MW(ε) Gas Cooled Fast Breeder Demonstration Plant*, GA-A-13045 (July 14, 1974).

2. R. E. Maerker et al., *Calibration of the Bonner Ball Neutron Detectors Used at the Tower Shielding Facility*, ORNL/TM-3465 (June 30, 1971).

3. C. E. Burgart and M. D. Emmett, *Monte Carlo Calculations of the Response Functions of Bonner Ball Neutron Detectors*, ORNL/TM-3739.

4. F. J. Muckenthaler, in *Applied Nuclear Physics Division Annual Report* for period ending September 10, 1956, pg. 199, ORNL-2081.

5. C. E. Burgart and M. D. Emmett, *Monte Carlo Calculations of the Response Functions of Bonner Ball Neutron Detectors*, ORNL/TM-3739.